

1 **Performance evaluation of deep learning and boosted trees for**  
2 **cryptocurrency closing price prediction**

3  
4  
5 **Authors**

6  
7 Azeez A. Oyedele  
8 Department of Law and Finance  
9 University of Bedfordshire, Luton Campus, United Kingdom  
10 Emails: [abiolaoyedele@yahoo.com](mailto:abiolaoyedele@yahoo.com) and [Azeez.Oyedele@beds.ac.uk](mailto:Azeez.Oyedele@beds.ac.uk)  
11

12 Anuoluwapo O. Ajayi (Corresponding Author)  
13 Big Data, Enterprise and Artificial Intelligence Laboratory (Big-DEAL)  
14 University of the West of England  
15 Frenchay Campus, Coldhambour Lane, Bristol, United Kingdom  
16 E-mail: [anuoluwapo.ajayi@uwe.ac.uk](mailto:anuoluwapo.ajayi@uwe.ac.uk)  
17

18 Lukumon O. Oyedele  
19 University of the West of England  
20 Frenchay Campus, Coldhambour Lane, Bristol, United Kingdom  
21 [ayolook2001@yahoo.co.uk](mailto:ayolook2001@yahoo.co.uk)  
22

23 Sururah A. Bello  
24 University of the West of England  
25 Frenchay Campus, Coldhambour Lane, Bristol, United Kingdom  
26 [Sururah.Bello@uwe.ac.uk](mailto:Sururah.Bello@uwe.ac.uk)  
27

28 Kudirat O. Jimoh  
29 Department of Information and Communication Technology,  
30 Osun State University, Nigeria.  
31 [kudirat.jimoh@uniosun.edu.ng](mailto:kudirat.jimoh@uniosun.edu.ng)  
32

33  
34  
35 **Corresponding author:** Anuoluwapo O. Ajayi  
36 **CA's email:** [anuoluwapo.ajayi@uwe.ac.uk](mailto:anuoluwapo.ajayi@uwe.ac.uk)  
37

## 38 Abstract

39  
40 *The emergence of cryptocurrencies has drawn significant investment capital in recent years with an exponential*  
41 *increase in market capitalization and trade volume. However, the cryptocurrency market is highly volatile and*  
42 *burdened with substantial heterogeneous datasets characterized by complex interactions between predictors, which*  
43 *may be difficult for conventional techniques to achieve optimal results. In addition, volatility significantly impacts*  
44 *investment decisions; thus, investors are confronted with how to determine the price and assess their financial*  
45 *investment risks reasonably. This study investigates the performance evaluation of a genetic algorithm tuned Deep*  
46 *Learning (DL) and boosted tree-based techniques to predict several cryptocurrencies' closing prices. The DL models*  
47 *include Convolutional Neural Networks (CNN), Deep Forward Neural Networks, and Gated Recurrent Units. The*  
48 *study assesses the performance of the DL models with boosted tree-based models on six cryptocurrency datasets from*  
49 *multiple data sources using relevant performance metrics. The results reveal that the CNN model has the least mean*  
50 *average percentage error of 0.08 and produces a consistent and highest explained variance score of 0.96 (on average)*  
51 *compared to other models. Hence, CNN is more reliable with limited training data and easily generalizable for*  
52 *predicting several cryptocurrencies' daily closing prices. Also, the results will help practitioners obtain a better*  
53 *understanding of crypto market challenges and offer practical strategies to lower risks.*

54  
55 **Keywords:** Artificial intelligence, Deep learning, Boosted trees, Optimization, Forecasting, Cryptocurrencies

## 56 57 1. Introduction

58 Cryptocurrencies have become a global phenomenon attracting a significant number of users due to their  
59 decentralization, immutability, and security. They are based on trust in technological infrastructure, allowing financial  
60 resources to be sent from anywhere with almost zero latency while network users provide the necessary authentication  
61 mechanisms. This new concept thus combines the advantages of transaction anonymity with the speed and  
62 convenience of electronic transactions without a central management institution. Over a few years, their increased  
63 transaction frequency, turnover, number of participants, and their structural self-organization have resulted in nearly  
64 indistinguishable complexity characteristics experienced in traditional financial markets, i.e., the foreign currency  
65 market (Forex), at the level of individual time series (Watorek et al., 2021).

66 Consequently, due to their increasing growth and popularity, they are now being used in official cash flows and the  
67 exchange of goods (Chowdhury et al., 2020). Similarly, due to the rapid flow of information and the availability of  
68 high-frequency data, machine learning (ML) techniques have gained popularity in the crypto market, especially price  
69 prediction, a critical step in financial decision-making related to portfolio optimization, risk evaluation, and trading.  
70 However, the cryptocurrency market is highly volatile and complex (Choo, 2015; Watorek et al., 2021; Zoumpikas  
71 et al., 2020), with substantial heterogeneous datasets characterized by complex interactions between predictors, which  
72 may be difficult for conventional ML techniques to achieve optimal results. Moreover, as a measure of price  
73 fluctuations, volatility significantly impacts trade strategies and investment decisions (Guo et al., 2018). Thus, it is  
74 essential to have models that can predict the crypto market accurately at par with the stock market. Furthermore,  
75 instant knowledge of price movements can lead to higher profits and lower investment risks for investors. Therefore,  
76 investigating the possibility of predicting several cryptocurrencies' closing prices using an optimal model  
77 configuration on training sets with significant peaks and drops in price missing and evaluating prediction accuracies  
78 on datasets from multiple data sources; is the motivation for this study.

79 Thus, this paper develops a decision support tool and contributes to the findings on comparing prediction models by  
80 making a focused comparison of Deep Learning (DL) and boosted tree-based techniques on six cryptocurrency  
81 datasets collected from three different data sources. More specifically, using the same optimal model configuration on  
82 different cryptocurrencies to investigate their robustness and resistance across imperfect training and testing datasets.  
83 A situation where training data is limited or covers only some of the phenomena in the training set has received  
84 relatively little attention in the literature. Few studies that used boosted tree-based techniques for modeling the crypto  
85 market either predict a famous and single cryptocurrency platform or use a single data source for training and testing  
86 the developed models (Sun et al., 2020). The DL techniques are selected because they are good at discovering intricate

87 structures in high-dimensional data (LeCun et al., 2015) and their remarkable problem-solving success in several  
88 domains. Furthermore, the predictive performance of DL techniques is benchmarked with three powerful boosted tree-  
89 based techniques that are scalable and robust for modeling complex data (Hastie et al., 2009; Sheridan et al., 2016).  
90 These attributes have resulted in them being incorporated into the Spark library for large-scale ML applications.

91 The rest of the paper is organized as follows: Section 2 presents the applications and benchmarking of Artificial  
92 intelligence (AI) and ML techniques for cryptocurrency price prediction. Then, Section 3 discusses the methodology,  
93 particularly the description of crypto datasets and data pre-processing techniques, genetic algorithms, DL, and boosted  
94 tree-based techniques. Finally, section 4 discusses prediction results, and Section 5 concludes the study.

## 95 **2. Related work**

96 Several quantitative research on financial market modeling has been carried out. Watorek et al. (2021) gave a detailed  
97 and comprehensive review of these studies and the statistical properties of the financial market price fluctuations.  
98 Based on its high trading activity by investors, many scholars are interested in modeling the crypto market or studying  
99 its linear and nonlinear dynamics. A few examples of such studies include using a time-scale multifractal approach to  
100 investigate the high frequency of Bitcoin prices and volume (Lahmiri & Bekiros, 2020a), detecting analysis of  
101 structural breaks and volatility spillovers (Canh et al., 2019), and modeling large abrupt price swings and long memory  
102 in volatility (Chaim & Laurini, 2019). Others involve examining long-range memory, distributional variation, and  
103 randomness of bitcoin volatility (Lahmiri et al., 2018) and analyzing the nonlinear correlations and multiscale  
104 characteristics of the cryptocurrency market (Watorek et al., 2021). Other interesting studies closely related to the  
105 present study are interested in forecasting cryptocurrency prices using artificial intelligence and advanced machine  
106 learning algorithms (Dutta et al., 2019; Kwon et al., 2019; Lahmiri & Bekiros, 2019; Lahmiri & Bekiros, 2020b;  
107 Mallqui & Fernandes, 2019; Miura et al., 2019; Zoumpiskas et al., 2020).  
108

109 Accordingly, in the last few years, the AI/ML community has deeply explored ML techniques (Table 1., i.e.,  
110 classification, regression, time series forecasting) to automatically generate profitable trading signals for the  
111 cryptocurrency market (Kristjanpoller & Minutolo, 2018). Most studies on quantitative cryptocurrency trading under  
112 classification aim to forecast the price trend of Bitcoin (BTC), a protocol based on a peer-to-peer network and public  
113 and private key cryptographic techniques. Bitcoin is also the natural base for other cryptocurrencies (Watorek et al.,  
114 2021), the leading and most capitalized (\$434 Billion) as of July 2022. For example, studies such as those from  
115 Alonso-Monsalve et al. (2020), Atsalakis et al. (2019), Ibrahim et al. (2021), Lahmiri and Bekiros (2020b), Mallqui  
116 and Fernandes (2019), Mudassir et al. (2020), Nakano et al. (2018), and Sun et al. (2020) addressed the prediction of  
117 the next-day direction (up or down) of Bitcoin (BTC) using classification models trained on historical data. These  
118 studies considered, amongst others, statistical and ML techniques such as Autoregressive Integrated Moving Average  
119 (ARIMA) (Ibrahim et al., 2021), k-nearest neighbor (Chowdhury *et al.*, 2020; Lahmiri & Bekiros, 2020), Artificial  
120 Neural Networks (ANN) (Chowdhury et al., 2020; Ibrahim et al., 2021; Lahmiri & Bekiros, 2020b; Mallqui &  
121 Fernandes, 2019; Mudassir et al., 2020), Logistic Regression (LR) (Borges & Neves, 2020; Chen et al., 2020), Random  
122 Forest RF) (Borges & Neves, 2020; Chen et al., 2020; Ibrahim et al., 2021; Sun et al., 2020), and Support Vector  
123 Machines (SVM) (Borges & Neves, 2020; Chen et al., 2020; Lahmiri & Bekiros, 2020b; Mallqui & Fernandes, 2019;  
124 Sun et al., 2020). Others include Bayesian Neural Networks (BNN) (Shah & Zhang, 2014), Gradient Boosting  
125 Machines (GBM) (Borges & Neves, 2020; Lahmiri & Bekiros, 2020; Sun et al., 2020), Extreme Gradient Boosting  
126 (XGB), neuro-fuzzy (Atsalakis et al., 2019), Long Short-Term Memories (LSTM) and Recurrent Neural Networks  
127 (Cherati et al., 20021; Mallqui & Fernandes, 2019; Mudassir et al., 2020), and Convolution Neural Networks (Alonso-  
128 Monsalve et al., 2020). For instance, Atsalakis et al. (2019) adopted neuro-fuzzy techniques to forecast the change in  
129 the direction of the BTC price and reported an increase of 71.21% in investment returns by the proposed model  
130 compared to the naive buy-and-hold strategy. Also, Alonso-Monclave et al. (2020) used hybrid Convolutional Neural  
131 Networks (CNN) and Long Short-Term Memory (LSTM) neural networks, CNN, ANN, and Radial Basis Neural

132 Networks (RBFNN) for intraday trend classification of BTC, Dash, Ether, Litecoin (LTC), Monero (XMR), and  
 133 Ripple (XRP), based on technical indicators.

134

135 Table 1. Previous studies using AI/ML approaches for cryptocurrency modeling

Reference	Algorithms	Data source	Remarks
Alonso-Monsalve <i>et al.</i> (2020)	CNN, hybrid CNN-LSTM, ANN, and RBFNN	Cryptocompare	intraday trend classification for BTC, DASH, Ether, LTC, XMR and XRP, based on technical indicators.
Atsalakis <i>et al.</i> (2019)	Neuro-Fuzzy	Bitcoincharts	to forecast the direction in the change of the BTC price.
Borges and Neves (2020)	LR, RF, SVM and GBM	Binance	BNB price trend predicting
Chen <i>et al.</i> (2020)	LR, RF, XGB, QDA, SVM and LSTM	CoinMarketCap	A classification problem to predict the sign change of BTC price
Cherati <i>et al.</i> 2021	LSTM	Binance	forecast daily closing price direction of BTC
Chowdhury <i>et al.</i> (2020)	Ensemble learning, GBM, ANNs, and K-NN	Not indicated	forecast the close (closing) price of the cryptocurrency index 30 and nine constituents of cryptocurrencies
Dutta <i>et al.</i> (2019)	ANN, LSTM, and GRU	Bitcoincharts	daily BTC price prediction
Guo <i>et al.</i> (2018)	GARCH, RF, Gaussian process, XGT, ElasticNet, LSTM, Temporal mixture models	Not indicated	short-term volatility prediction of BTC price.
Ibrahim <i>et al.</i> (2021)	ARIMA, Prophet, RF, RF Lagged-Auto-Regression, and FFDNN	Coinmarketcap	predict market movement direction of BTC
Jang and Lee (2018)	BNN and linear models	Bitcoincharts	analyzing BTC processes
Kristjanpoller and Minutolo (2018)	GARCH and ANN	Not indicated	predict the price volatility of BTC
Kwon <i>et al.</i> (2019)	LSTM and GBM	Bithumb	a classification problem for the price trend (price-up or price-down) of BTC, ETH, XRP, BCH, LTC, DASH, and Ethereum Classic.
Lahmiri and Bekiros (2019)	LSTM and GRNN	Not indicated	for price prediction in Dash, XRP, and BTC.
Lahmiri and Bekiros (2020b)	SVR, GRP, RT, kNN, ANN, BRNN and RBFNN	Bitcoin intraday price data	comparatively evaluate ML techniques in forecasting high-frequency price level of BTC.
Mallqui and Fernandes (2019)	Ensembles, RNNs, ANN, SVM	Bitcoincharts and Quandl	compare different ensembles and neural networks to classify BTC price direction and predict closing price.
Huang <i>et al.</i> (2019)	Decision trees	Investing	BTC returns prediction
Miura <i>et al.</i> (2019)	LSTM, ANN, Ridge, SVM, and GRU	Bitstamp	to predict BTC price volatility
Mudassir <i>et al.</i> (2020)	ANN, Stacked ANN, LSTM, SVM	Bitinfocharts	for predicting BTC price movements and prices in short and medium terms
Nakano <i>et al.</i> (2018)	DNN	Poloniex	to predict price direction on BTC 15-min time intervals using prices and technical indicators
Peng <i>et al.</i> (2018)	GARCH with SVR	Altcoin Charts	predict volatilities of BTC, ETH, and DASH
Poongodi <i>et al.</i> (2020)	Linear regression and SVM	Etherchain.org	Ether coin close price prediction.
Shah and Zhang (2014)	BNN	Okcoin	to predict the BTC price variation.
Sun <i>et al.</i> (2020)	Light GBM, SVM, RF	Investing	forecast the price trend (falling, or not falling) of cryptocurrency markets
Zoumpikas <i>et al.</i> (2020)	CNN, LSTM, Stacked LSTM, Bidirectional LSTM, and GRU	Poloniex	predict the ETH closing price in a short period

136

137 They reported that the hybrid CNN-LSTM architecture outperformed other methods considered. Similarly, Ibrahim et  
138 al. (2021) compared ARIMA, Prophet, Random Forest, Random Forest Lagged-Auto-Regression, and feed-forward  
139 deep neural networks (FFDNN); they reported that FFDNN achieved the highest accuracy of 54% compared to other  
140 predictive models. Also, Borges and Neves (2020) compared LR, RF, SVM, and GBM with ensemble voting for the  
141 BNB coin market and risk value prediction. They reported that the ensemble voting method, on average, outperformed  
142 other learning algorithms with an accuracy of 56.28%. Finally, Chen et al. (2020) compared LR, SVM, LSTM, XGB,  
143 Linear discriminant analysis, Quadratic discriminate analysis, and RF for the Bitcoin price trend prediction. The  
144 LSTM model obtained the highest accuracy of 67.2%. Also, Cherati et al. (2021) used an LSTM model to forecast the  
145 daily closing price direction of the BTC/US and obtained an accuracy of 76.83% on the testing data.

146 Regarding regression modeling, studies such as those from Chowdhury *et al.* (2020), Dutta *et al.* (2019), Lahmiri and  
147 Bekiros (2019), Poongodi *et al.* (2020), and Zoumpikas *et al.* (2020) developed regression models for cryptocurrency  
148 price prediction. Such studies employed ML techniques, i.e., linear regression and SVM for Ether coin price prediction  
149 (Poongodi *et al.*, 2020), ANN for cryptocurrencies, i.e., BTC, ETH, Dash, price prediction (Chowdhury *et al.*, 2020;  
150 Dutta *et al.*, 2019), GBM (Chowdhury *et al.*, 2020), k-NN (Chowdhury *et al.*, 2020), and deep learning LSTM and  
151 GRU (Dutta *et al.*, 2019; Kwon *et al.*, 2019; Lahmiri & Bekiros, 2019; Zoumpikas *et al.*, 2020) for predictive model  
152 development. For instance, Dutta et al. (2019) compared Recurrent Neural Networks (RNN) and ANNs to predict  
153 daily BTC prices, using daily data from January 2010 to June 2019. In the study, feature selection was based on the  
154 Variance Inflation Factor (VIF), and the authors reported the performance of RNNs over ANNs on this task. Similarly,  
155 Lahmiri and Bekiros (2019) benchmarked LSTM with Generalized Regression Neural Networks (GRNN) for BTC  
156 price prediction and reported that LSTM performed better with a smaller Root Mean Square Error (RMSE:  $2.75 \times$   
157  $10^3$ ) compared to  $8.80 \times 10^3$  for GRNN. Also, Poongodi et al. (2020) adopted linear regression and SVM models for  
158 Ethereum (ETH) closing price prediction and concluded that the SVM method had higher accuracy (96.06%) than the  
159 LR method (85.46%). Similarly, Zoumpikas (2020) utilized deep learning algorithms to predict the closing price of  
160 the Ethereum cryptocurrency and reported a Squared-R of predicted versus the actual ETH/USD data to a degree of  
161 more than 60%. Finally, Chowdhury *et al.* (2020) used ANN, GBM, KNN, and ensemble learning methods to forecast  
162 the closing price of the cryptocurrency index 30 and nine constituents of cryptocurrencies and reported the highest  
163 RMSE obtained for BTC as 32.863 with the GBM model.

164  
165 In terms of time series prediction, Jang and Lee (2018) used Bayesian Neural Networks to predict the log price and  
166 the log volatility of Bitcoin price and obtained MAPE values equal to 0.0198 and 0.6302 for log price and log volatility,  
167 respectively. The authors also compared the predictive performance of BNN with a Support Vector Regression (SVR)  
168 and linear models. Kristjanpoller and Minutolo (2018) integrated Generalized Auto-regressive Conditional  
169 Heteroskedasticity (GARCH) and ANN with Principal Component Analysis (PCA) to predict Bitcoin's price volatility.  
170 They reported that the proposed model could capture price volatility to mitigate exposure to financial risk. Also, Peng  
171 et al. (2018) evaluated the predictive performance of a hybrid GARCH and Support Vector Regression model in  
172 estimating the volatility of three cryptocurrencies and three currencies. Similarly, Guo et al. (2018) formulated  
173 probabilistic temporal mixture models to capture autoregressive dependence in price volatility history. They  
174 benchmarked the predictive performance of the proposed models with some conventional techniques and concluded  
175 that the proposed model had the lowest RMSE in price volatility prediction. Also, Miura et al. (2019) predicted the  
176 future volatility values based on past samples using ANN, GRU, LSTM, SVM, and Ridge Regression techniques.  
177 They concluded that the Ridge Regression had the overall best performance.

178  
179 Consequently, previous studies employing AI/ML techniques have aimed to model the cryptocurrency market for  
180 improved decision-making regarding investments with higher returns and lower risk (Borge & Neves, 2020;  
181 Kristjanpoller & Minutolo, 2018). This interest is associated with increasing efforts being expended by researchers  
182 and financial organizations to minimize financial risks. However, the predictive performance of current frameworks  
183 still needs improvements, as evidenced by several cryptocurrency price modeling studies aimed at improving  
184 forecasting methods for profitable investment decisions (Ibrahim et al., 2021; Huang et al., 2019; Jang & Lee, 2018;

185 Kristjanpoller & Minutolo, 2018; Peng et al., 2018; Watorek et al., 2021). Furthermore, financial investors need  
186 efficient strategies to reduce financial risk resulting from the increased complexity characteristics observed across  
187 most financial markets (Watorek et al., 2021). Traditional ML techniques require manual feature extraction from  
188 massive datasets to transform data into internal forms to enhance ML models' predictive ability (LeCun et al., 2015)  
189 for guaranteed optimal results. This limitation, in addition to the specific issue each ML model has. For instance, the  
190 logistic regression model has difficulty capturing nonlinear and local relationships among dependent and independent  
191 variables. Similarly, despite their ability to learn from data and fault tolerances, ANNs can suffer from uncontrolled  
192 convergence speed and local optima. Also, Bayesian Neural Networks and SVMs have computational complexity  
193 issues. Also, decision trees can have high variance across samples, making predictions and probabilities unstable for  
194 new cases. Besides these challenges, modern financial markets are characterized by a rapid flow of information, high-  
195 frequency data, nonlinear interactions, and complex characteristics (Watorek et al., 2021), which may be difficult for  
196 conventional ML techniques to achieve optimal results.

197  
198 Also, in modeling cryptocurrencies and benchmarking different ML models' performance, most existing studies  
199 considered a single data source of historical data for training, validating, and testing their models. In addition, most  
200 used ML models to predict famous and single cryptocurrency platforms, i.e., BTC price (Atsalakis et al., 2019; Chen  
201 et al., 2020; Lahmiri & Bekiros, 2020; Shah & Zhang, 2014), ETH (Zoumpikas et al., 2020), and BNB (Borges &  
202 Neves, 2020). However, other cryptocurrencies, i.e., LTC, Dogecoin (DOGE), and Stellar (XLM), are among the top  
203 10 currencies with the potential to be adopted in financial institutions. Akyildirim et al. (2021) also opined that these  
204 other cryptocurrencies had attracted relatively less attention. Therefore, besides the established cryptocurrencies, it is  
205 worth investigating ML models' robustness on less famous ones to offer a suitable strategy for their price prediction  
206 and understand their overall price dynamics. Similarly, the robustness of an optimal model configuration on several  
207 cryptocurrencies and performance on the different testing datasets require an assessment, especially models' sensitivity  
208 to training sets, where peaks and drops in prices are not adequately represented, has hitherto received little academic  
209 attention. Therefore, constructing robust predictive models to accurately forecast prices for multiple cryptocurrencies  
210 is a significant business challenge for probable investors and government agencies. Accordingly, a robust technique  
211 is desirable to improve prediction ability to enhance the prediction of cryptocurrencies' closing prices for improved  
212 financial investments.

213  
214 Therefore, deep learning techniques are adopted in this study because of their advantage in discovering intricate  
215 structures in high-dimensional data, their ability to represent complex data, and their remarkable problem-solving  
216 successes in several domains (LeCun et al., 2015). Though, deep learning architectures, i.e., CNN, LSTM, GRU,  
217 DFNN, have been actively used for cryptocurrency price, volatility, and return predictions in recent years (Alonso-  
218 Monsalve et al., 2020; Dutta et al., 2019; Guo et al., 2018; Ibrahim et al., 2021; Mallqui & Fernandes, 2019; Nakano  
219 et al., 2018; Zoumpikas et al., 2020). However, it is noted that in studies such as those from Alonso-Monsalve et al.  
220 (2020) and Nakano et al. (2018), CNN and DNN techniques were used primarily for trend (price direction)  
221 classification problems. Instead, this present study utilizes both techniques for estimating a real-valued variable  
222 (closing price). Also, it is observed that Dutta et al. (2019) and Zoumpikas et al. (2020) adopted deep learning  
223 techniques, i.e., CNN and GRU, to predict the closing price of either BTC or ETH. In contrast, this current study  
224 adopts the same configurations of CNN, DFNN, and GRU architectures to predict the daily closing prices of multiple  
225 cryptocurrencies from multiple data sources. Also, the predictive abilities of the proposed all-inclusive and optimal  
226 deep learning models are benchmarked with a few key powerful boosted tree techniques in GBM, Adaboost, and XGB  
227 using standard metrics from the literature.

228  
229  
230  
231  
232

### 233 3. Methodology

#### 234 3.1. Dataset and Data preprocessing

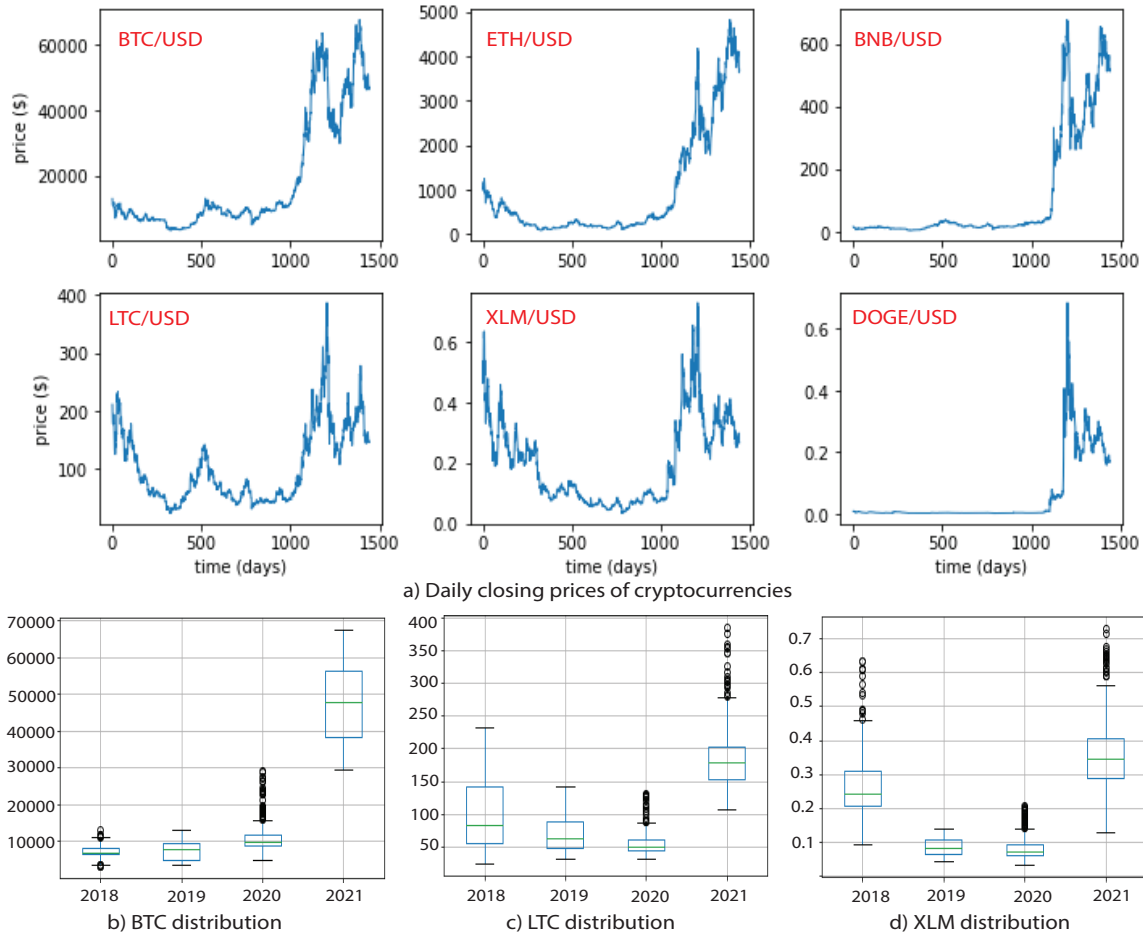
235 The study collected datasets from Yahoo finance, UK Investing, and Bitfinex to investigate the robustness of  
236 prediction models in terms of how they respond to patterns in multiple data sources. For example, the dataset from  
237 Yahoo finance is for training and validating the models, while other datasets are for testing the prediction models. The  
238 Yahoo finance dataset for the six cryptocurrencies (BTC-USD, ETH-USD, BNB-USD, LTC-USD, XLM-USD, and  
239 DOGE-USD) covers the duration between January 1, 2018, to December 31, 2021 (1442 observations). UK Investing  
240 dataset covers from July 1, 2021, to March 2, 2022 (245 observations). Also, the Bitfinex dataset for the six  
241 cryptocurrencies is from January 1, 2021, to July 6, 2021 (187 observations). More importantly, validating models on  
242 different datasets helps guarantee that they do not fit data-specific features. Each dataset has five features, namely, the  
243 closing price (Close), highest price (High), lowest price (Low), opening price (Open), and the daily cryptocurrency  
244 volume (Volume). In addition, additional features are created, i.e., weighted average (using “Price” as values and  
245 “year” as weights) and technical indicators that may impact prices, which include simple moving average (SMA) and  
246 exponential moving average (EMA). The rationale for selecting SMA is to allow a model to recognize trends by  
247 smoothing the data more efficiently. At the same time, EMA facilitates the dampening of the effects of short-term  
248 oscillations. The significant difference between SMA and EMA is that EMA assigns a greater weight to recent data  
249 and reacts faster to recent price variations. Furthermore, these technical indicators are calculated using different  
250 periods, i.e., day 3, day 10, and day 20.

251 Fig 1a depicts the price exhibiting nonlinear dynamical traits for the six cryptocurrencies versus time from January 1,  
252 2018, to December 31, 2021. For instance, in Fig. 1a, BTC indicates that the price significantly rose in late 2020  
253 (around 13/11/2020, approximately at index 1048 on the graph). Similarly, for ETH, a significant increase in closing  
254 price becomes noticeable around 02/02/2021, approximately at index 1129 on the graph. Also, a significant increase  
255 in the BNB price is at index 1136 on the graph, i.e., 09/02/2021. Similarly, Figs 1a and Table 2 present the summary  
256 statistics of cryptocurrencies (Yahoo finance) from 2018 to 2021. Though world financial markets do not work  
257 simultaneously due to different time zones, most work around the clock, and only temporary price fluctuations caused  
258 by the human factor are noticeable. Thus, to study this temporary price fluctuation, the percentage changes in  
259 cryptocurrency prices during the day were calculated, and moderate changes ranging from 0.05% to 1% were  
260 discovered. Thus, the time zones have little or no effect on the cryptocurrency market. Furthermore, these  
261 cryptocurrencies from the three datasets (Yahoo finance, UK Investing, Bitfinex) are similar and have identical  
262 distributions.

263  
264 Again, there are no missing values in the datasets; however, there are noticeable outliers, as depicted in the box plots  
265 containing the information to identify their distribution. For instance, the closing prices for BTC in 2018 and 2020  
266 have outliers (Fig. 1b). Also, LTC in 2020 and 2021 (Fig. 1c) has outliers, and XLM has outliers in 2018, 2020 and  
267 2021 (Fig. 1d). Nevertheless, outliers are kept in the predictive modeling phase since they carry meaningful  
268 information and deleting them could cause substantial information loss. However, the normalization technique is  
269 adopted to transform raw data into a form where the features are all uniformly distributed, i.e., standardizing the  
270 features with their mean and standard deviation to address the dominant features and outliers. Nevertheless,  
271 understanding the effect of the training data size on the model performance is critical to advancing the knowledge  
272 about its generalization ability, specifically in investigating the robustness of models where specific insights are not  
273 in training sets. Thus, two scenarios are presented in training the prediction models and tuning their parameters. The  
274 purpose is to investigate the training set size dimensions’ effects on prediction quality. The first (Scenario A) divides  
275 each cryptocurrency dataset from Yahoo Finance into training (1154 days, i.e., from 01/01/2018 - 28/02/2021) and  
276 test (i.e., 305 days: 01/03/2021 - 31/12/2021). Here prominent peaks in cryptocurrency prices are missing from the  
277 training set. Scenario B divides each cryptocurrency dataset from Yahoo finance into training (1240 days, i.e., from  
278 01/01/2018 to 25/05/2021) and test set (i.e., 219 days: 26/05/2021-31/12/2021). Thus, scenario B has sufficient peaks  
279 and lows in prices captured in the training set. For instance, Fig 2. depicts the two scenarios illustrated with BNB/USD,

280 where higher spikes are not part of the training set (Scenario A), and some of these spikes are incorporated in the  
 281 training set (Scenario B).

282



283  
 284 Fig. 1. Cryptocurrency trends and distributions  
 285  
 286

287 Table 2. Dataset description- Yahoo Finance

		Open	High	Low	Volume	WP	SMA3	SMA10	SMA20	EMA10	Price
BTC	min	3236.3	3275.4	3191.3	2.9e+9	8.9	3244.0	3397.0	3524.7	3425.1	3236.8
	mean	18408.8	16054.0	15160.1	2.6e+10	50.5	18405.3	18317.8	18199.8	18319.5	18429.6
	max	67549.7	68789.6	66382.1	3.5e+11	185.1	66511.3	64698.9	63149.3	64411.4	67566.8
LTC	min	23.5	23.8	22.8	1.9e+8	0.1	23.6	24.6	27.4	25.3	23.5
	mean	102.7	106.6	98.3	2.8e+9	0.2	102.6	102.8	103.1	102.8	96.34
	max	387.9	413.0	345.3	1.7e+10	1.1	374.4	347.2	316.0	342.2	386.5
ETH	min	84.3	85.3	82.8	9.5e+8	0.2	84.7	89.2	97.3	90.5	84.3
	mean	933.5	965.8	897.0	1.3e+10	2.6	933.2	926.7	917.0	926.5	935.1
	Max	4174.6	4891.7	4718.0	8.4e+10	13.2	4727.8	4655.8	4531.5	4621.4	4812.1
BNB	min	4.5	4.6	4.2	9.3e+3	0.0	4.6	4.7	5.0	4.8	4.5
	mean	108.6	113.0	103.9	8.8e+8	0.3	108.5	107.3	105.5	107.3	108.9
	max	676.3	690.9	634.5	1.7e+10	1.9	655.3	643.1	614.7	637.0	675.7
DOGE	min	0.0	0.0	0.0	2.1e+6	0.0	0.0	0.0	0.0	0.0	0.0
	mean	0.1	0.1	0.1	1.0e+9	0.0	0.1	0.1	0.1	0.1	0.1
	max	0.7	0.7	0.6	6.9e+10	0.0	0.6	0.6	0.5	0.5	0.7
XLM	min	0.0	0.0	0.0	1.9e+7	0.0	0.0	0.0	0.0	0.0	0.0
	mean	0.2	0.2	0.2	5.1e+8	0.0	0.2	0.2	0.2	0.2	0.2
	max	0.7	0.8	0.7	1.0e+10	0.0	0.7	0.7	0.6	0.7	0.7

288



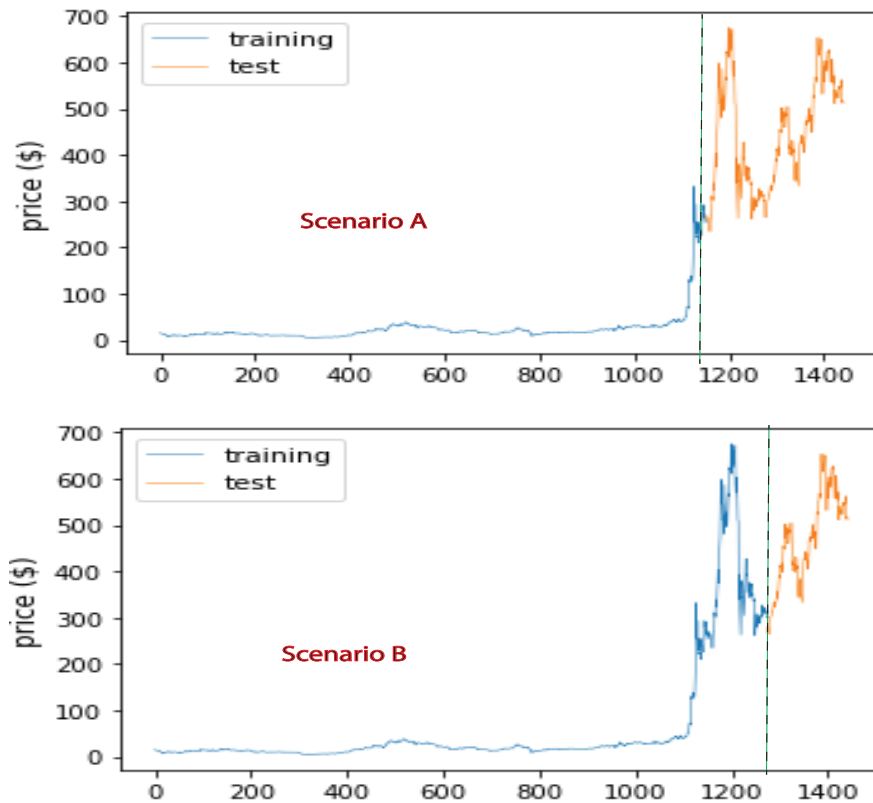


Fig 2. Illustrating the two scenarios (A and B) with respect to training data sizes

290  
291  
292

### 293 3.2. Boosted tree-based technique

294 This technique represents ensembles of multiple weak trees to improve robustness over a single predictive model. The  
295 three boosted tree-based techniques considered are briefly described.

#### 296 3.2.1. Adaptive boosting

297 AdaBoost or ADAB is generally less susceptible to overfitting problems and works by fitting a series of weak learners  
298 (i.e., decision trees) on repeatedly modified versions of data. Predictions from the weak learners are then combined  
299 through a weighted majority vote to produce the final prediction. The data modifications at each boosting iteration  
300 apply weights  $w_1, w_2, \dots, w_N$  to training samples, with initial weights at  $w_j=1/N$ . Thus, the first step merely trains a  
301 weak learner on the original data. Then, the sample weights are individually modified for each successive iteration,  
302 and the learning algorithm is reapplied to the reweighted data. At a given step, the training examples with incorrect  
303 predictions at the previous step will have their weights increased. In contrast, those predicted correctly will have their  
304 weights decreased. As iterations progress, the difficult to predict examples will receive more attention. Thus, each  
305 subsequent weak learner is forced to concentrate on examples previously missed in the sequence (Hastie et al., 2009).  
306 Mathematically, given a training set with  $m$  samples. Let  $t(j)$  be the actual cryptocurrency price of sample  $j$  for  $j=1, 2,$   
307  $\dots, k$ . ADAB generates  $L$  sub-regressors ( $l_p$ ) and trains each regressor on a sampled sub-dataset  $D_p, p=1, 2, \dots, L$  of  
308 the same size as the original training set. For each regressor  $l_p$ , the normalized estimation error for sample  $j, j=1, 2, \dots,$   
309  $k$ , is denoted as  $e_p^j = \frac{|t^j - l_p(x^j)|}{\max_{j=1}^k |t^j - l_p(x^j)|}$ , and the estimation error of  $l_p$  computed using  $\beta_p = \sum_{j=1}^k \omega_p^j e_p^j$ . Then, the  
310 weight of sample  $j$  is updated as

311

$$\omega_p^j = \frac{\omega_{p-1}^j}{Z_{p-1}} \left( \frac{\beta_{p-1}}{1 - \beta_{p-1}} \right)^{1 - e_{p-1}^j} \quad (1)$$

312

313

314

315

316

317

318

319

320

321

322

323

324

325

326

327

Where  $Z_{p-1}$  is a normalizing constant, intuitively, by Equation (1), the samples with a significant estimation error in the last iteration are assigned a significant sampling weight in the next iteration. Thus, during the training process, ADAB reduces estimation errors by paying attention to samples that are difficult to predict accurately. The final trained AdaBoost regressor is a weighted regressor  $l(x)$  overall  $L$  sub-regressors defined as  $l(x) = \sum_{p=1}^L \ln\left(\frac{1-\beta_p}{\beta_p}\right) l_p(x)$ , where the weight  $\ln\left(\frac{1-\beta_p}{\beta_p}\right)$  of regressor  $l_p$  decreases with estimation errors,  $\beta_p$ , i.e., regressors with smaller estimation errors contribute more to the final regressor  $l(x)$ . The genetic algorithm (Algorithm 1) was used to tune three ADAB parameters: the number of estimators ( $n\_estimators$ ), loss, and the learning rate ( $learning\_rate$ ). A slower learning rate takes much time and has more probability of converging or being stuck in an undesirable local minimum. At the same time, a higher one makes the learning jump over minima. Thus, this study considers the range (1.0 to 1.3) for the learning rate since this range was observed to be more appropriate during validation. The *number of estimators* is another parameter affecting the model's accuracy, as a larger value may lead to overfitting; hence, the hyperparameter sample space was limited to between 65 to 75. Additionally, the "loss" parameter was set to 'square' since it gave the best results during validation. Finally, the optimal configuration for ADAB was derived by computing the average value of these parameters for the repeated trials (6) representing the number of cryptocurrencies as depicted in Algorithm 1.

328

### 3.2.2. Gradient Boosting Machines

329

330

331

332

333

334

GBMs (Friedman, 2001) derive a strong learner by combining an ensemble of weak learners (i.e., decision trees) interactively. For a training dataset,  $S$  defined as  $S = \{x_j, y_j\}_1^n$ , the goal of the algorithm is to approximate function  $F^*(x)$  to give  $F(x)$ , i.e., mapping instances of  $x$  to output values  $y$  by minimizing the expected loss function,  $L(y, F(x))$ . Thus, the algorithm builds an additive approximation of  $F^*(x)$  as a weighted sum of functions defined as  $F_k(x) = F_{k-1}(x) + \omega_k h_k(x)$  where  $\omega_k$  represents the weight of the  $k$ th function,  $h_k(x)$ . In constructing the approximation, a constant approximation of  $F^*(x)$  is first derived as

335

$$F_0(x) = \underset{\alpha}{\operatorname{argmin}} \sum_{j=1}^n L(y_j, \alpha) \quad (2)$$

336

With subsequent models minimizing

337

$$\omega_k h_k(x) = \underset{\omega, h}{\operatorname{argmin}} \sum_{j=1}^n L(y_j, F_{k-1}(x_j) + \omega h(x_j)) \quad (3)$$

338

339

340

341

Where each model,  $h_k$ , is seen as a greedy step in a gradient descent optimization for  $F^*$ , and each  $h_k$  is trained on a new dataset  $S = \{x_j \gamma_{kj}\}_{j=1}^n$  with residuals,  $\gamma_{kj}$ , derived as

342

$$\gamma_{kj} = \left\{ \frac{\partial L(y_j F(x))}{\partial F(x)} \right\}_{F(x)=F_{k-1}(x)} \quad (4)$$

343

344

345

346

347

348

The value of  $\omega_k$  is consequently computed by solving a linear search optimization problem, which suffers from overfitting if the iterative process is not correctly regularized (Friedman, 2001). Nevertheless, when controlling the additive process of the gradient boosting algorithm, several regularization parameters are often considered. One way to regularize the algorithm is to apply a shrinkage factor,  $\vartheta$ , to reduce each gradient descent step  $F_k(x) = F_{k-1}(x) + \vartheta \omega_k h_k(x)$ ,  $\vartheta \in [0, 1.0]$ . Also, regularization can be achieved by limiting the complexity of the trained models, i.e., by limiting the depth of the trees or the minimum number of instances necessary for node splitting.

349 The genetic algorithm was used to tune three GBM parameters: the number of estimators ( $n\_estimators$ ), tree depth  
 350 ( $max\_depth$ ), and the learning rate ( $learning\_rate$ ). Boosting may potentially overfit when large estimators are used;  
 351 hence, this range was limited to between 65 to 75, a very conservative value compared to examples provided in the  
 352 literature (Hastie et al., 2009). The tree depths between 3 and 8 are known to give the best results (Hastie et al., 2009).  
 353 Moreover, stumps with only one split allow for no variable interaction effects. Thus, a tree depth range of between 3  
 354 to 6 was used to allow a reasonable interaction. Also, the learning rate ( $\alpha$ ) represents the speed of learning achieved  
 355 by the model. This study considers  $0.80 \leq \alpha \leq 1.20$ , due to the small number of trees used and to derive a  
 356 computationally feasible model. Using a genetic algorithm (GA) specified in Algorithm 1, a reasonable number of  
 357 estimators (70), tree depth (4), and learning rate (0.999) were similarly derived (Table 3).  
 358

### 359 3.2.3. Extreme Gradient Boosting

360 The XGB (Chen & Guestrin, 2016) represents an ensemble tree model utilizing the gradient boosting framework  
 361 designed to be highly scalable and improve gradient boosting. This algorithm also exhibits better capability and higher  
 362 computation efficiency when dealing with overfitting. XGB constructs an additive expansion of the objective function  
 363 by decreasing a variation of the loss function,  $L'$ , used to control the complexity of the trees and defined as Equation  
 364 (5):

$$365 \quad L' = \sum_{j=1}^n L(y_j, F(x_j)) + \sum_{k=1}^m \theta(h_k) \quad (5)$$

366 Where  $\theta(h) = \gamma Z + \frac{1}{2} \lambda \|\eta\|^2$ ,  $Z$  represents the number of leaves in the tree, and  $\eta$  represents the output scores of  
 367 leaves. This loss function is incorporated into the split criterion of decision trees leading to a pre-pruning procedure.  
 368 The value of  $\gamma$  controls the minimum loss reduction gain required to split the internal node; however, higher values of  
 369  $\gamma$  result in simpler trees. An additional regularization parameter, known as shrinkage,  $\lambda$ , can be employed to reduce  
 370 step size in the additive expansion. Also, the complexity of trees can be controlled using other approaches, i.e., the  
 371 depth of the trees. Tree complexity reduction ensures models are trained faster with less storage space requirement.  
 372 Furthermore, randomization techniques (random subsamples and column subsampling) are available to reduce  
 373 overfitting and training speed. Also, three XGB parameters: the learning rate, number of estimators ( $n\_estimators$ ),  
 374 and the maximum depth of the tree ( $max\_depth$ ), were tuned using the GA method while setting other parameters at  
 375 their default values. The optimal configurations (Table 3) obtained after averaging the best configurations from the  
 376 six cryptocurrencies are  $learning\_rate$  (1.135),  $n\_estimators$  (63), and  $max\_depth$  (5).  
 377

## 378 3.3. Deep Learning techniques

379 These are a new branch of ML techniques that have gained widespread recognition and are successfully deployed in  
 380 various applications. A brief discussion on DL architectures considered is as follows.  
 381

### 382 3.3.1. Deep feedforward neural networks

383 The deep feedforward neural network (DFNN) is the typical DL model for hierarchically learning complex and  
 384 abstract data representations. This learning process transmits data through multiple transformation layers (Ajayi et al.,  
 385 2020). The typical architecture of DFNN has three layers, namely, input layer, hidden layer, and output layer, in which  
 386 each layer has several interconnected processing units. In DFNN, each layer utilizes a nonlinear transformation on its  
 387 input to produce its output. The neural network is assumed to consist of  $N$  layers. The output signal of the  $l^{\text{th}}$  layer is  
 388 expressed as in Equation (6).

$$389 \quad d_j^l = f(w_j^T a_j^{l-1} + b_j), \quad l = 1, 2, 3, \dots, N \quad (6)$$

390 Where  $f$  is the activation function;  $w_j^T$  is the weight vector which indicates the effect of all units in the same hidden  
 391 layer;  $a_j^{l-1}$  defines the output signal of the  $l-1^{\text{th}}$  layer;  $b_j$  represents the bias parameter of the  $j^{\text{th}}$  unit in the  $l^{\text{th}}$  layer.

392 Since this problem is a regression problem, the rectified linear unit (ReLU) was selected as the activation function in  
393 the DFNN architecture to transfer input signals to the output because it is computationally efficient and will ensure  
394 better performance of models. Also, ReLU is nearly linear and easy to optimize with gradient-based methods. In  
395 addition, it can learn faster with networks consisting of many layers, thus allowing the training of deep neural networks  
396 without an unsupervised pre-training (Glorot et al., 2011). Mathematically, ReLU is expressed as  $f(x) =$   
397  $\begin{cases} 0 & \text{for } x < 0 \\ x & \text{for } x \geq 0 \end{cases}$ . Furthermore, the Mean square error (MSE) was used to evaluate the model's prediction accuracy while  
398 training the DFNN model. MSE is normally expressed as  $MSE = \frac{1}{n} \sum_{j=1}^n (o_j - y_j)^2$ , where  $n$  is the number of samples  
399 in a training set;  $o_j$  represent the measured values and  $y_j$  represent predicted values. In constructing the DFNN model,  
400 the number of hidden layers was first derived. Generally, increasing the number of hidden layers imply longer  
401 computational time and larger storage of training parameters. However, considering the datasets and computational  
402 cost, it was observed that a neuron network architecture with only two hidden layers could reasonably model the  
403 cryptocurrency problem in this study. Therefore, the architecture consisted of an input layer, two hidden layers, and  
404 an output layer. The Root Mean Square Propagation (RMSprop) optimizer was adopted for the MSE loss minimization  
405 since its combination with ReLU attained the lowest training MSE at 100 epochs. In addition, the RMSProp optimizer  
406 made the entire network converge faster. Also, the dropout method (Srivastava et al., 2014) was used to deal with the  
407 overfitting problem. The drop rate used is 0.1%. Choosing an optimal number of neurons for each hidden layer is  
408 critical to the performance of a neural network. Thus, the GA method was used to tune the parameters: the number of  
409 neurons in each Dense layer (two layers were used), the number of epochs, and the training batch size (Table 3), to  
410 derive an optimal model configuration for the cryptocurrencies.

### 411 412 3.3.2. Gated recurrent units

413 The gated recurrent units (GRUs) by Cho et al. (2014) use gates to control information flow, and they are introduced  
414 to solve the vanishing gradient problem with the standard RNNs. Though GRU is similar to LSTM, however GRU  
415 network has an update gate that combines the forget and input gates of LSTM into a single update gate. In addition,  
416 the cell state and the hidden state are further merged in GRU, thus, making its structure simpler, more efficient in the  
417 training phase, and, in general, train faster than LSTM. Furthermore, GRUs are known to outperform LSTMs in tasks  
418 with a limited number of data instances. The linking of the writes and forget gates in the GRU update gate imposes a  
419 restraint on the cell state to coordinate the writes and forgets. Alternatively, rather than doing selective writes and  
420 selective forgets, a selective overwrites, i.e., setting the forget gate equal to 1 minus the write gate, is done using  
421 Equation (7):

$$422 \quad h_t = (1 - z_t) \odot h_{t-1} + z_t \odot \tilde{h}_t \quad (7)$$

423 Where  $z_t$  denotes the update gate, and  $h_t$  represents the memory content. An element-wise multiplication,  $\odot$ , is applied  
424 to  $(1 - z_t)$  and the preceding memory content  $h_{t-1}$  in (6), followed by an element-wise multiplication on  $z_t$  and the  
425 current memory content  $\tilde{h}_t$ , thus resulting in a summation of two element-wise multiplications. Usually, the GRU unit  
426 structure consists of the update gate ( $z_t$ ), reset gate ( $r_t$ ), and the current memory content ( $\tilde{h}_t$ ). These gates permit the  
427 storage of values in the GRU unit memory for a certain amount of time and then carry these values forward, when  
428 required, to the current state to update at a future date. The update gate multiplies and adds the input  $x_t$  and the output  
429 from the previous unit  $h_{t-1}$  and is used to tackle the vanishing gradient problem when training models. A sigmoid  
430 function is used to obtain outputs between 0 and 1. The reset gate regulates how much of the past information to  
431 disregard. The current memory content is where  $x_t$  is multiplied by  $W$  and  $r_t$  is multiplied by  $h_{t-1}$  elementwise, with a  
432 tanh activation function applied to the final summation. The final GRU unit memory,  $h_t$ , holds the information for the  
433 current unit, which is passed on to the network. The GRU architecture consists of a single layer of GRU unit driven  
434 by the input sequence and the activation function, set as ReLU. Also, RMSprop was used to optimize the training and  
435 GA (Algorithm 1) to tune its parameters (number of neurons in GRU and Dense layers, epochs, and training batch  
436 size). As a result, the optimal values (Table 3) obtained are the number of neurons (13 each) for GRU and Dense  
437 layers, epochs (80), and training batch size (43), respectively.

438

### 439 3.3.3. Convolutional neural networks (1-D)

440 CNNs typically consist of a set of successive convolutional and subsampling layers, one or more hidden layers, and  
441 an output layer. The first two types of layers are combined to extract high-level feature vectors in one dimension. The  
442 feature vectors are later handled by the fully connected multilayer perceptron and output layers. Also, an activation  
443 function is usually applied to the resulting field following the convolution operation. The ReLU activation function is  
444 computationally efficient for CNNs (Dahl et al., 2013), in addition, it is favored because it preserves the magnitude of  
445 positive signals as they travel forward and backward through the network (LeCun et al., 2015). Finally, convolution  
446 filters are applied across all inputs simultaneously, which allows them to identify correlated patterns across multiple  
447 input variables or the results of previous convolutions. The advantage of CNN is that the training is relatively easy  
448 because its number of weights is less than that of a fully connected architecture, thus, facilitating the easy extraction  
449 of essential features. Formally, the 1D forward propagation from convolution layer l-1 to the input of a neuron in layer  
450 l is expressed as in Equation (8):

$$451 \quad x_k^l = b_k^l + \sum_{i=1}^{N_{l-1}} \text{conv1D}(w_{ik}^{l-1}, s_i^{l-1}) \quad (8)$$

452 Where the scalar bias of the k<sup>th</sup> neuron  $b_k^l$ , the output of the i<sup>th</sup> neuron at layer l-1  $s_i^{l-1}$ , and the kernel from the i<sup>th</sup>  
453 neuron at layer l-1 to the k<sup>th</sup> neuron at layer l  $w_{ik}^{l-1}$  are used to determine the input  $x_k^l$  at layer l. Also, the conv1D (..)   
454 function represents a 1-D convolution without zero padding on the boundaries. Finally, the intermediate output of the  
455 neuron,  $y_k^l$ , which is a function of the input,  $x_k^l$ , and the output of the neuron  $s_k^l$  at layer l (a subsampled version of  $y_k^l$ )  
456 is as defined in Equation (9):

$$457 \quad y_k^l = f(x_k^l) \text{ and } s_k^l = y_k^l \downarrow ss \quad (9)$$

458  
459 Where  $s_k^l$  stands for the output of the k<sup>th</sup> neuron of the layer, l, and “ $\downarrow ss$ ” represents the down-sampling operation  
460 with a scalar factor, ss. In achieving the utmost computational efficiency, the study adopts a simple 1-D CNN with  
461 only one CNN layer and one MLP layer. Moreover, most recent studies employing 1D CNN applications use compact  
462 (with 1–2 hidden CNN layers) configurations. Also, since CNN models learn very quickly, a dropout layer (Srivastava  
463 et al., 2014) was used to help slow down the learning process and facilitate better generalization. Furthermore, ReLU,  
464 a computationally efficient activation function for CNNs (Dahl et al., 2013), and RMSprop were used in learning  
465 optimization. Finally, four parameters: the number of filters, the number of neurons in the dense layer, the number of  
466 epochs, and the batch size for the six cryptocurrencies, were tuned using Algorithm 1. The optimal values of these  
467 parameters are filters (10), units (13), epochs (82), and batch size (52).

### 468 3.4. Genetic algorithms

470 Genetic algorithms (GA) (Goldberg, 2006) provide the opportunity to randomly search the hyper-parameter space  
471 while utilizing the previous results to direct the search. Each hyperparameter to optimize is encoded as a single gene  
472 for each individual. A range is then defined for each gene to eliminate searching for disinterested areas in the  
473 hyperparameter space. Initially, the population is generated by selecting each gene from a uniform random  
474 distribution, then each individual's fitness is evaluated. Each generation is then formed using selection, crossover, and  
475 mutation predicated on individuals having the highest fitness scores from the previous generation. This procedure  
476 represents a single generation of random search followed by a result-driven search based on the best previous  
477 individuals. A selection operation is performed by removing individuals from the population with a fitness value  
478 smaller than their generation's average fitness. Then, the next generation is created by performing the crossover and  
479 mutation operations on the remaining individuals. The *GAsearchCV* function in Python's sklearn-genetic-opt is used  
480 to optimize the hyperparameters by minimizing the RMSE of the prediction models. The algorithm used to derive the  
481 optimal hyperparameters for the deep learning and tree-based methods is depicted in Algorithm 1, and the function  
482 code *genetic\_parameters\_tune* defined in the Code Ocean platform <https://codeocean.com/capsule/0499275/tree/v1>

483

484 After deriving the best parameters of the models on each cryptocurrency dataset, the average value of these parameters  
 485 was then determined as the optimal model configuration. Table 3 presents the optimal configurations of predictive  
 486 models' hyperparameters for cryptocurrencies considered in this study. Some important *GAsearchCV* arguments used  
 487 are:

- 488 1) population: This represents the initial amount of hyperparameters candidates to generate randomly, thus was set  
 489 to 10 in this study.
- 490 2) generations: The argument represents the number of iterations the algorithm will make and creates a new  
 491 population every generation. It was set to 5 in this study.
- 492 3) crossover\_probability: The probability that a crossover occurs in a particular mating. A crossover probability of  
 493 0.9 was used in this study.
- 494 4) mutation\_probability: The probability that an already fixed individual suffers a random change in some of its  
 495 hyperparameters values. A mutation probability of 0.05 was used to limit the search radius for faster convergence.
- 496 5) param\_grid: a dictionary with keys as names of hyperparameters and their values, i.e., a list of parameters for a  
 497 typical GBM model can be expressed as:  
 498 param\_grid = {'learning\_rate': Continuous (0.8, 1.3), 'max\_depth': Integer (3, 6), 'n\_estimators': Integer (65, 75)}

500 Table 3. Parameter bounds, optimal parameters for each cryptocurrency, and the average value for models

Model	Parameter	Range	Cryptocurrency						Average
			BTC	ETH	BNB	LTC	XLM	DOGE	
ADA	learning_rate	[1.00 - 1.30]	1.283	1.286	1.246	1.218	1.030	1.223	1.214
	n_estimators	[65-75]	65	73	70	74	75	75	72
	loss	Square	-	-	-	-	-	-	-
GBM	max_depth	[3-6]	3	3	6	4	3	6	4
	learning_rate	[0.80 - 1.30]	1.192	1.001	0.868	1.048	1.016	0.864	0.999
	n_estimators	[65 - 75]	70	71	65	70	70	74	70
XGB	max_depth	[3 - 6]	6	6	4	6	3	5	5
	learning_rate	[0.80 - 1.30]	1.271	1.137	0.839	1.115	1.149	1.298	1.135
	n_estimators	[60 - 70]	63	60	67	63	62	65	63
MLP	units (each of the 2 layers)	[14 - 19]	15	18	14	15	15	17	16
	batch_size	[40 - 50]	43	41	43	47	50	47	45
	epochs	[80 - 90]	85	84	84	87	80	80	83
GRU	units (each of the 2 layers)	[11 - 14]	11	13	13	14	13	11	13
	batch_size	[42 - 45]	42	43	42	44	43	42	43
	epochs	[76 - 84]	80	84	76	76	79	82	80
CNN	filters	[9 - 12]	10	12	10	9	9	9	10
	units	[10 - 14]	10	13	14	13	14	12	13
	batch_size	[44 - 54]	54	52	51	49	54	50	52
	epochs	[75-85]	83	85	77	81	81	84	82

501

### 502 3.5. Performance evaluation

503 Consequently, to finally evaluate the performance of prediction models on testing datasets (yahoo finance; validating  
 504 sets -UK Investing and Bitfinex), statistical analysis involving standard metrics is conducted to quantify the extent to  
 505 which the predicted closing prices are close to the corresponding true values. These metrics are briefly described:  
 506

- 507 1) Nash-Sutcliffe coefficient of Efficiency (NSE) provides a more direct measure of the agreement between the  
 508 observed closing price and predicted values, and it is expressed as in Equation (10).

$$509 \quad NSE = 1 - \left[ \frac{\sum_{j=1}^n (o_j - y_j)^2}{\sum_{j=1}^n (o_j - \bar{o})^2} \right] \quad (10)$$

510 Where  $y_j$  represents forecasts,  $o_j$  represents corresponding measured outputs, and  $\bar{o}$  represents the mean of  
 511 the measured output. A value of NSE closer to 1 implies that the model can satisfactorily reproduce the

512 observed cryptocurrency closing price. NSE = 1.0 indicates a perfect match of the model predictions to the  
 513 observed values.  
 514

### ALGORITHM 1

---

```

INPUT: X1,6 // cryptocurrency datasets (BTC, ETH, BNB, LTC, XLM, DOGE)
OUTPUT: xgb_opt, gbm_opt, ada_opt, gru_opt, mlp_opt, cnn_opt // optimal parameter values

Xtrain1,6, Xtest1,6 = split_data (X1,6, proportions)
ytrain1,6, ytest1,6 = split_data (y1,6, proportions)

# p1, p2, p3, etc represents parameters, i.e., max_depth, learning rate, filters, units, batch size, epochs,

# Set bounds for parameters
# LBound – lower bound of a parameter, UBound – maximum value of a parameter
xgb_grid = {p1: LBound, UBound, p2: (LBound, UBound), p3: LBound, UBound }
gbm_grid = {p1: LBound, UBound, p2: (LBound, UBound), p3: LBound, UBound }
ada_grid = {p1: LBound, UBound, p2: (LBound, UBound), p3: LBound, UBound }
gru_grid = {p1: LBound, UBound, p2: (LBound, UBound), p3: LBound, UBound }
mlp_grid = {p1: LBound, UBound, p2: (LBound, UBound), p3: LBound, UBound }
cnn_grid = {p1: LBound, UBound, p2: (LBound, UBound), p3: LBound, UBound, p4: LBound, UBound,}

# Set up the genetic solver for each of the predictive model, i.e., XGB, GBM, ADA, GRU, MLP & CNN
xgb_ = GAsSearchCV (solver =xgb, cv=3, scoring='mse', population=10, generations=5, param_grid=xgb_grid, ...)
gbm_ = GAsSearchCV (solver =gbm, cv=3, scoring='mse', population=10, generations=5, param_grid=gbm_grid, ...)
ada_ = GAsSearchCV (solver =ada, cv=3, scoring='mse', population=10, generations=5, param_grid=ada_grid, ...)
gru_ = GAsSearchCV (solver =gru, cv=3, scoring='mse', population=10, generations=5, param_grid=gru_grid, ...)
mlp_ = GAsSearchCV (solver =mlp, cv=3, scoring='mse', population=10, generations=5, param_grid=mlp_grid, ...)
cnn_ = GAsSearchCV (solver =cnn, cv=3, scoring='mse', population=10, generations=5, param_grid=cnn_grid, ...)

# Fit the generic solver on the data to find optimum parameters
FOR i=1 TO 6 DO
  xgb_fit (Xtrain[i], ytrain[i])
  gbm_fit (Xtrain[i], ytrain[i])
  ada_fit (Xtrain[i], ytrain[i])
  gru_fit (Xtrain[i], ytrain[i])
  mlp_fit (Xtrain[i], ytrain[i])
  cnn_fit (Xtrain[i], ytrain[i])

  # Store the best parameters used to fit models for each dataset Xtrain
  xgb_dict[{xgb_best[p1],xgb_best[p2],xgb_best[p3]}] = {mse[ytest[i], xgb_predict(Xtest[i])]} # append dictionary
  gbm_dict[{gbm_best[p1],gbm_best[p2],gbm_best[p3]}] = {mse[ytest[i], gbm_predict(Xtest[i])]}
  ada_dict[{ada_best[p1],ada_best[p2],ada_best[p3]}] = {mse[ytest[i], ada_predict(Xtest[i])]}
  gru_dict[{gru_best[p1],gru_best[p2],gru_best[p3]}] = {mse[ytest[i], gru_predict(Xtest[i])]}
  mlp_dict[{mlp_best[p1],mlp_best[p2],mlp_best[p3]}] = {mse[ytest[i], mlp_predict(Xtest[i])]}
  cnn_dict[{cnn_best[p1],cnn_best[p2],cnn_best[p3],cnn_best[p4]}] = {mse[ytest[i], cnn_predict(Xtest [i])]}
END DO

# Compute average values of these parameters as the optimal parameter configurations of models for all datasets
xgb_opt= mean(DataFrame(xgb_dict)) # three parameters tuned
gbm_opt= mean(DataFrame(gbm_dict)) # three parameters tuned
ada_opt= mean(DataFrame(ada_dict)) # compute the means of two numerical parameters tuned
gru_opt= mean(DataFrame(gru_dict)) # Averages of three parameters tuned
mlp_opt= mean(DataFrame(mlp_dict)) # Averages of the three parameters tuned
cnn_opt= mean(DataFrame(cnn_dict)) # Averages of four tuned parameters

```

515  
 516  
 517 2) Explained Variance Score (EVS) compares the variance within the expected outcomes to the variance in the  
 518 model error. This metric essentially represents the amount of variation (dispersion) in the original dataset  
 519 that a model can explain, and it is estimated as follows.

$$520 \quad EVS(o, y) = 1 - \frac{var(o - y)}{var(o)} \quad (11)$$

521 Where y is the estimated target output, o represents the corresponding target output, and var is the variance  
 522 (i.e., the square of the standard deviation). The best possible score is 1.0, and lower values are worse for  
 523 prediction models.

524  
525  
526  
527  
528  
529  
530  
531  
532  
533  
534  
535  
536  
537  
538  
539  
540  
541  
542  
543  
544  
545  
546  
547  
548  
549  
550

- 3) The  $t$ -test illustrates the overestimation or underestimation of the data at a 95% significance level. The  $t$ -test is calculated (Equation 12) as the ratio of  $SS_1$  and  $SS_2$

$$t = \frac{SS_1}{SS_2} \quad (12)$$

where  $SS_1 = \frac{\sum_{j=1}^n (o_j - y_j)}{n}$ , is the average of the differences between the measured,  $o_j$ , and the estimated,  $y_j$ , cryptocurrency price values, and  $SS_2 = \sqrt{\frac{\sum_{j=1}^n |(o_j - y_j) - SS_1|^2}{n-1}}$ . Where a population of  $n > 120$  and the absolute value of  $t \leq 1.96$ , there is no statistically significant difference between the observed and calculated data at a 95% confidence level. Values of  $t$  close to zero indicate a higher accuracy. For a positive  $t$ -test value, the measured value is not statistically greater than the estimated one (at 95% confidence level). Conversely, for a negative  $t$ -test value, the calculated value is not significantly greater than the measured value at the confidence level of 95%.

- 4) The Mean Absolute Percentage Error (MAPE) measure determines the percentage of error per prediction and is defined in Equation (13):

$$MAPE = \frac{1}{n} * \sum_{j=1}^n \left| \frac{y_j - o_j}{o_j} \right| * 100 \quad (13)$$

The smaller the MAPE, the better the performance of the model. MAPE is relevant in finance as gains and losses are often measured in relative values. In addition, it is valuable for calibrating products' prices since customers are sometimes more sensitive to relative variations than absolute variations.

To further investigate the performance of the prediction models, graphical techniques were employed to determine the degree of agreement between forecasts and measured closing price values. Also, the graphical methods facilitate qualitative and subjective evaluation. Finally, all the models were developed using the Keras high-level DL library and TensorFlow as the low-level backend. All experimental work was carried out on a personal computer (2.9 GHz 6- Core Intel with 32 GB of RAM and a hard disk memory of 1TB). Also, sample outputs presented in the following sections can also be simulated by interested readers using the source code available on Code Ocean (<https://doi.org/10.24433/CO.2359079.v1>).

#### 4. Results and discussion

The performance evaluation of models using statistical indicators: NSE, EVS,  $t$ -test, and MAPE on each cryptocurrency for the two scenarios is summarized in Tables 4 and 5. The results (Table 4A: Scenario A) indicate that the average EVS for the six cryptocurrencies ranges between 0.60 and 0.94. However, DL techniques obtained a more significant percentage (between 88% to 94% on average), indicating that they have accounted for the total variance in the observed data. This result contrasts those from boosted tree-based models having average EVS values ranging from 0.60 to 0.62, thus, struggling in their predictions, especially for ETH, BNB, and DOGE, due to insights not captured in training sets. Similarly, in comparing the robustness of models with different data sources, DL models, especially CNN and GRU, produce consistent and higher EVS values ( $0.76 \leq EVS \leq 0.99$ ) compared to boosted tree-based models, which are extremely low in some cases ( $0.03 \leq EVS \leq 0.50$ ) for ETH and DOGE. Thus, boosted tree-based models exhibit unreliable predictions for these cryptocurrencies when certain information is missing from the training set. Nonetheless, in Table 4B (Scenario B), there is an improvement in predictions from most models as the EVS for predictions ranges between 0.75 and 1. A high value of EVS indicates more significant similarities between the measured and predicted values. A perfect model has  $EVS = 1$ . Thus, predictions (on average) from CNN and GRU models (Scenarios A and B) for most cryptocurrencies are considered ideal since  $0.95 \leq EVS \leq 0.96$  and acceptable



566  $0.91 \leq EVS < 0.93$  (for DFNN). However, predictions (on average) from the boosted tree-based models (Scenarios  
567 A and B) can be considered very good ( $0.78 \leq EVS \leq 0.80$ ).

568 The MAPE metric quantifies how close the models' predictions are to the actual (closing price) values. The smaller  
569 the MAPE value (closer to zero), the closer the predictions are to the true values and the better the predictive models'  
570 performance. As shown in Tables 4 and 5, the predictive models yield smaller MAPE values (Scenario A). For  
571 example, the CNN model has the smallest average MAPE of 9%, followed by GRU with an average MAPE of 11%,  
572 GBM (average MAPE of 17%), DFNN (average MAPE of 18%), XGB (average MAPE of 18%), and ADAB (average  
573 MAPE of 18%). However, the MAPE indexes of the closing prices estimated by the models for all cryptocurrencies  
574 on the three testing sets are within 3% to 12% (Table 4: Scenario B), implying a high prediction accuracy of models.  
575 In addition, all the predictive models obtain the absolute (t-test) value,  $t \leq 1.96$ , for all cryptocurrencies, except DFNN  
576 ( $1.99 \leq t\text{-test} \leq 2.02$ ) for DOGE (Scenario A). Thus, for most predictive models, there is no statistically significant  
577 difference between the observed and predicted closing price at a 95% confidence level, as depicted in Table 4.  
578 Also, the predictive models' fit expressed as NSE obtained in Scenario A ranged from -3.09 to 0.99 (Boosted tree-  
579 based models) and -1.35 to 0.99 (DL techniques). Similarly, NSE (Scenario B) ranged from 0.16 to 1.00 (Boosted  
580 tree-based techniques) and -0.37 to 0.99 (DL techniques). The NSE higher values indicate better model performance.  
581 Thus, the mean Nash–Sutcliffe coefficient obtained by combining both scenarios for all models ranges between 0.45  
582 and 0.88 (Table 5), with the highest mean Nash–Sutcliffe coefficient value obtained by CNN (0.88) followed by GRU  
583 (0.85). The least overall mean of the Nash–Sutcliffe coefficient was obtained by ADAB (0.45).

584 Furthermore, as a means of visual inspection, the fitness of the prediction models was evaluated using residual plots  
585 to examine the prediction bias of models (Scenario A) on the UK Investing datasets. For the DL techniques, most  
586 cryptocurrencies have residuals randomly distributed around the zero horizontal lines, except CNN (BTC and DOGE),  
587 DFNN (DOGE), and GRU (BTC, ETH, and BNB). Thus, the residuals (Fig. 3), for most cryptocurrencies, exhibited  
588 no defined patterns and satisfied the assumption that the residuals have a constant variance. However, residuals from  
589 the boosted tree-based counterparts (Fig. 4) were neither symmetric to the origin nor randomly distributed. Hence,  
590 their inability to learn from limited examples and generalize some degree of knowledge in predicting closing prices.  
591 Figs. 5-8 further demonstrate the daily variations of the observed and predicted closing prices for the UK investing  
592 and Yahoo finance datasets (Scenarios A and B). As shown in Fig. 5. (Scenario A), the DL-based models' predictions  
593 correspond well with the observed values, i.e., the overall trend or pattern is entirely consistent, showing a good  
594 correlation, especially for CNN models. Thus, CNN produces more accurate and robust results for the different  
595 cryptocurrency datasets. However, by outputting high error margins, the boosted tree-based models underfit some  
596 cryptocurrency datasets (i.e., ETH, BNB, and DOGE). Thus, they do not present a representative picture of the  
597 relationship between predictions and measured values for these cryptocurrencies. Consequently, the results confirm  
598 the boosted trees-based limitations when vital information is missing from training sets. However, all six predictors  
599 performed well and produced more accurate results on the validation datasets as more training data, capturing peaks  
600 and drops in prices, were used. This realistic prediction performance is captured in Table 4: Scenario B (all validation  
601 sets- Yahoo finance, UK investing, and Bitfinex) and Figs 7 and 8 for the UK investing datasets.

603 The performance of DL and boosted tree-based models is also graphically evaluated using Taylor's diagram (Fig. 9  
604 and 10 - Scenario A). The diagram graphically displays a statistical summary of how well the predictions from the  
605 models correspond to the observed values in terms of their correlation coefficient, center RMSE, and standard  
606 deviation. From Fig. 9, the position of colored numbers (i.e., 1, 2, 3, 4, 5 and 6) quantifies how close the predictions  
607 from the models (i.e., ADAB, GBM, XGB, GRU, DFNN, and CNN) are to the observed closing prices for each  
608 cryptocurrency. The red dotted arc in the diagram represents the observed standard deviation at the point  
609 marked "*observed*" on the x-axis. Predictions from boosted trees are farther from the point marked "*observed*" for  
610 ETH-USD, BNB-USD, LTC-USD, and DOGE-USD, compared to predictions from the DL techniques.  
611

Table 4. Statistical performance of prediction models

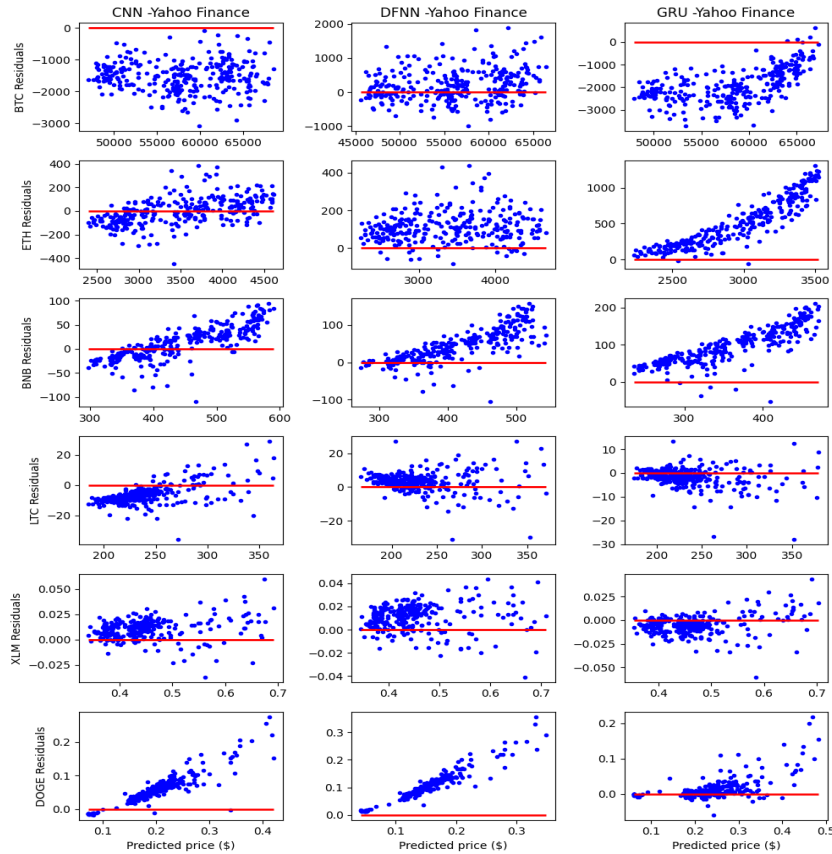
Scenario A (Table 4A)																				
Model	Statistical Index	BTC			ETH			BNB			LTC			XLM			DOGE			Mean
		Data1	Data2	Data3	Data1	Data2	Data3	Data1	Data2	Data3	Data1	Data2	Data3	Data1	Data2	Data3	Data1	Data2	Data3	
XGB	EVS	0.97	0.98	0.99	0.03	0.50	0.50	0.08	0.53	0.55	0.79	0.92	0.92	0.97	0.98	0.98	0.03	0.10	0.10	0.61
	MAPE	1%	2%	2%	25%	17%	17%	24%	21%	20%	2%	2%	2%	2%	3%	3%	65%	56%	56%	18%
	t-test	0.00	-0.04	-0.08	1.43	0.88	0.89	1.14	0.88	0.93	0.32	0.21	0.21	0.18	-0.06	-0.12	1.79	1.27	1.27	0.62
	NSE	0.97	0.98	0.99	-1.96	0.11	0.09	-1.11	0.16	0.16	0.77	0.92	0.92	0.97	0.98	0.98	-3.09	-1.37	-1.37	0.01
GBM	EVS	0.97	0.95	0.95	0.03	0.50	0.50	0.19	0.59	0.59	0.80	0.92	0.92	0.94	0.97	0.97	0.04	0.13	0.13	0.62
	MAPE	1%	3%	3%	24%	16%	16%	21%	18%	18%	2%	2%	1%	2%	3%	3%	65%	56%	56%	17%
	t-test	-0.07	0.05	-0.01	1.38	0.85	0.86	1.13	0.88	0.88	0.31	0.20	0.20	0.39	0.08	-0.01	1.78	1.30	1.30	0.64
	NSE	0.97	0.95	0.95	-1.83	0.14	0.14	-0.85	0.27	0.27	0.78	0.92	0.92	0.93	0.97	0.97	-3.02	-1.34	-1.34	0.04
ADAB	EVS	0.97	0.99	0.99	0.03	0.49	0.49	0.06	0.47	0.47	0.76	0.91	0.91	0.98	0.99	0.99	0.04	0.13	0.13	0.60
	MAPE	1%	1%	1%	25%	16%	16%	28%	23%	23%	2%	1%	1%	2%	2%	64%	55%	55%	18%	
	t-test	-0.03	0.06	0.08	1.42	0.85	0.86	1.36	1.00	1.00	0.34	0.23	0.23	0.15	0.06	-0.01	1.77	1.29	1.29	0.66
	NSE	0.97	0.99	0.99	-1.93	0.11	0.11	-1.70	-0.07	-0.07	0.74	0.91	0.91	0.98	0.99	0.99	-2.98	-1.32	-1.32	-0.04
GRU	EVS	0.98	0.98	0.98	0.76	0.89	0.89	0.81	0.84	0.86	0.99	0.99	0.99	0.98	0.98	0.98	0.91	0.91	0.91	0.92
	MAPE	4%	2%	2%	14%	12%	12%	20%	29%	28%	1%	3%	2%	2%	4%	4%	6%	24%	24%	11%
	t-test	-2.53	-0.5	-0.5	1.57	1.19	1.19	2.01	1.90	2.10	-0.42	0.54	0.57	-0.49	-0.93	-0.78	0.49	1.28	1.28	0.44
	NSE	0.87	0.98	0.98	0.17	0.73	0.73	0.03	0.26	0.27	0.99	0.98	0.98	0.98	0.96	0.96	0.89	0.75	0.75	0.74
DFFN	EVS	0.99	0.98	0.99	0.99	0.98	0.99	0.83	0.68	0.70	0.98	0.95	0.96	0.98	0.98	0.98	0.75	0.54	0.54	0.88
	MAPE	1%	2%	2%	3%	8%	5%	9%	42%	43%	2%	5%	4%	3%	3%	39%	79%	79%	18%	
	t-test	0.46	0.38	0.4	1.38	1.29	0.98	0.99	2.07	2.13	0.53	0.73	0.60	1.00	0.17	0.18	1.99	2.02	2.02	1.07
	NSE	0.99	0.98	0.98	0.96	0.95	0.98	0.67	-0.69	-0.69	0.97	0.92	0.95	0.96	0.98	0.98	-0.25	-1.35	-1.35	0.44
CNN	EVS	<b>0.99</b>	<b>0.99</b>	<b>0.99</b>	<b>0.97</b>	<b>0.99</b>	<b>0.99</b>	<b>0.90</b>	<b>0.88</b>	<b>0.90</b>	<b>0.97</b>	<b>0.98</b>	<b>0.98</b>	<b>0.98</b>	<b>0.98</b>	<b>0.97</b>	<b>0.82</b>	<b>0.82</b>	<b>0.82</b>	<b>0.94</b>
	MAPE	3%	2%	2%	3%	3%	3%	6%	20%	19%	3%	4%	3%	3%	3%	22%	34%	34%	9%	
	t-test	-3.17	0.50	0.40	0.00	0.50	0.59	0.38	1.51	1.68	-0.88	-0.75	-0.6	1.06	0.09	0.18	1.31	1.46	1.46	0.32
	NSE	0.92	0.98	0.98	0.97	0.99	0.99	0.89	0.61	0.62	0.95	0.97	0.97	0.96	0.98	0.97	0.52	0.43	0.43	0.84
Scenario B (Table 4B)																				
XGB	EVS	0.99	0.99	0.99	0.95	0.99	0.99	0.98	0.99	0.99	0.98	0.99	0.99	0.96	0.98	0.98	0.81	0.98	0.98	0.97
	MAPE	1%	1%	1%	3%	2%	2%	3%	3%	3%	1%	1%	1%	2%	3%	3%	8%	8%	8%	3%
	t-test	0.10	0.14	0.16	0.44	0.25	0.27	-0.17	-0.14	-0.12	-0.25	-0.05	-0.02	0.24	0.08	-0.03	-0.5	-0.44	-0.44	-0.03
	NSE	0.99	0.99	0.99	0.94	0.99	0.99	0.97	0.99	0.99	0.98	0.99	0.99	0.95	0.98	0.98	0.76	0.98	0.98	0.97
GBM	EVS	0.98	0.98	0.98	0.94	0.98	0.98	0.95	0.98	0.98	0.99	0.99	0.99	0.95	0.98	0.98	0.69	0.97	0.97	0.96
	MAPE	1%	2%	2%	3%	3%	3%	5%	5%	5%	1%	1%	1%	2%	3%	3%	10%	9%	9%	4%
	t-test	-0.34	-0.02	-0.02	-0.06	-0.11	-0.16	-0.32	-0.19	-0.19	0.2	-0.03	-0.09	0.16	-0.07	-0.14	-0.57	-0.46	-0.46	-0.16
	NSE	0.98	0.98	0.98	0.94	0.98	0.98	0.95	0.98	0.98	0.99	0.99	0.99	0.95	0.98	0.98	0.58	0.97	0.97	0.95
ADAB	EVS	0.99	0.99	0.99	0.96	0.99	0.99	0.99	1.00	1.00	0.99	1.00	1.00	0.96	0.99	0.99	0.61	0.95	0.95	0.96
	MAPE	1%	1%	1%	2%	2%	2%	1%	3%	3%	1%	1%	1%	2%	2%	15%	16%	16%	4%	
	t-test	0.08	0.05	0.06	0.34	0.29	0.31	-0.44	-0.36	-0.32	0.38	0.16	0.15	0.22	0.08	-0.02	-1.07	-0.73	-0.73	-0.09
	NSE	0.99	0.99	0.99	0.96	0.99	0.99	0.99	1.00	1.00	0.99	1.00	1.00	0.96	0.99	0.99	0.16	0.93	0.93	0.94
GRU	EVS	0.96	0.94	0.94	0.99	0.99	0.99	0.99	1.00	1.00	0.98	0.98	0.98	0.98	0.98	0.98	0.97	0.98	0.98	<b>0.98</b>
	MAPE	2%	5%	5%	3%	2%	2%	3%	3%	4%	1%	3%	2%	2%	3%	3%	0.06	8%	8%	4%
	t-test	0.79	0.93	0.97	-0.98	-0.37	-0.4	1.8	0.87	0.9	0.16	0.51	0.43	1.21	0.29	0.39	1.78	-0.2	-0.2	0.49
	NSE	0.93	0.89	0.89	0.98	0.99	0.99	0.97	0.99	0.99	0.98	0.97	0.98	0.94	0.98	0.98	0.87	0.98	0.98	0.96
DFFN	EVS	0.99	0.98	0.98	0.95	0.97	0.98	1.00	0.97	0.97	0.98	0.97	0.98	0.98	0.98	0.98	0.97	0.75	0.75	0.95
	MAPE	3%	4%	4%	6%	6%	6%	3%	14%	13%	2%	3%	2%	1%	3%	3%	16%	67%	67%	12%
	t-test	2.27	1.49	1.52	1.52	1.16	1.47	2.09	-2.23	-2.12	1.10	-0.22	-0.04	0.54	-0.33	-0.24	5.44	2.13	2.13	0.98
	NSE	0.92	0.95	0.95	0.83	0.94	0.94	0.98	0.84	0.85	0.95	0.97	0.98	0.97	0.98	0.98	0.19	-0.37	-0.37	0.75
CNN	EVS	<b>0.99</b>	<b>0.99</b>	<b>0.99</b>	<b>0.99</b>	<b>0.97</b>	<b>0.97</b>	<b>0.99</b>	<b>0.98</b>	<b>0.99</b>	<b>0.99</b>	<b>0.98</b>	<b>0.99</b>	<b>0.98</b>	<b>0.98</b>	<b>0.98</b>	<b>0.94</b>	<b>0.96</b>	<b>0.96</b>	<b>0.98</b>
	MAPE	1%	3%	3%	4%	11%	11%	7%	15%	16%	3%	4%	3%	5%	3%	7%	13%	13%	7%	
	t-test	0.65	1.08	1.00	2.26	2.00	1.87	3.73	2.94	3.68	-2.5	-1.13	-1.04	-3.37	-0.43	-0.49	-1.23	1.07	1.07	0.62
	NSE	0.98	0.97	0.97	0.94	0.86	0.86	0.88	0.85	0.85	0.92	0.96	0.98	0.69	0.98	0.98	0.84	0.91	0.91	0.91

Data1 -Yahoo finance, Data2- UK Investing, Data3 - Bitfinex

615 Table 5. Summary of models' performance in the two scenarios

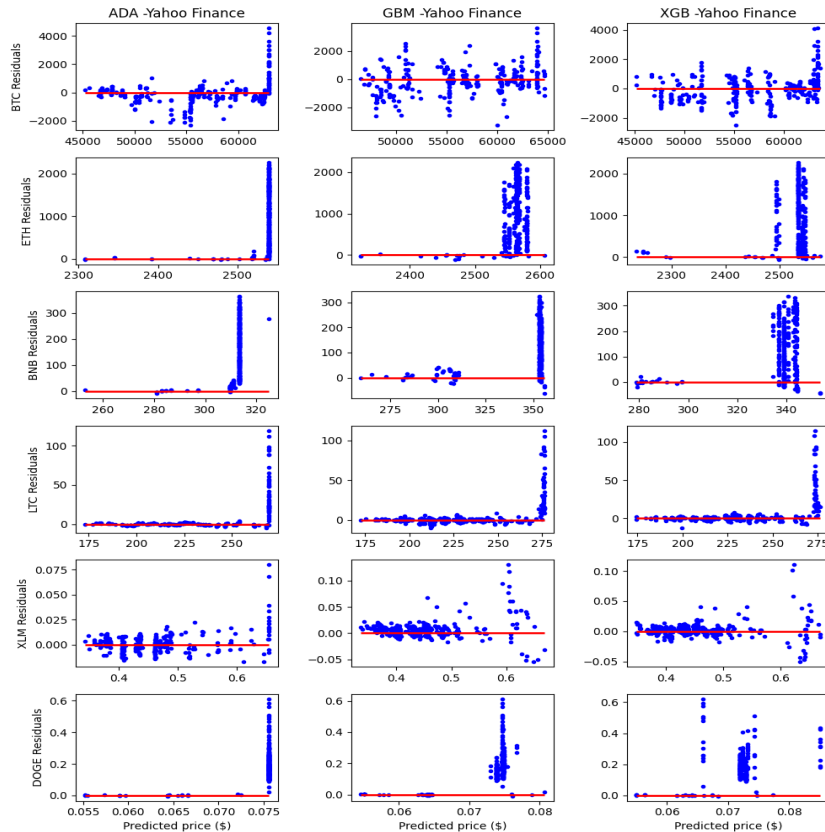
Model	Metric	Scenario A (mean)	Scenario B (mean)	Overall mean
XGB	EVS	0.61	0.97	0.79
	MAPE	0.18	0.03	0.11
	t-test	0.62	-0.03	0.30
	NSE	0.01	0.97	0.49
GBM	EVS	0.62	0.96	0.79
	MAPE	0.17	0.04	0.11
	t-test	0.64	-0.16	0.24
	NSE	0.04	0.95	0.50
ADAB	EVS	0.60	0.96	0.78
	MAPE	0.18	0.04	0.11
	t-test	0.66	-0.09	0.29
	NSE	-0.04	0.94	0.45
GRU	EVS	0.92	0.98	0.95
	MAPE	0.11	0.04	0.08
	t-test	0.44	0.49	0.47
	NSE	0.74	0.96	0.85
DFNN	EVS	0.88	0.95	0.92
	MAPE	0.18	0.12	0.15
	t-test	1.07	0.98	1.03
	NSE	0.44	0.75	0.60
CNN	EVS	0.94	0.98	0.96
	MAPE	0.09	0.07	0.08
	t-test	0.32	0.62	0.47
	NSE	0.84	0.91	0.88

616



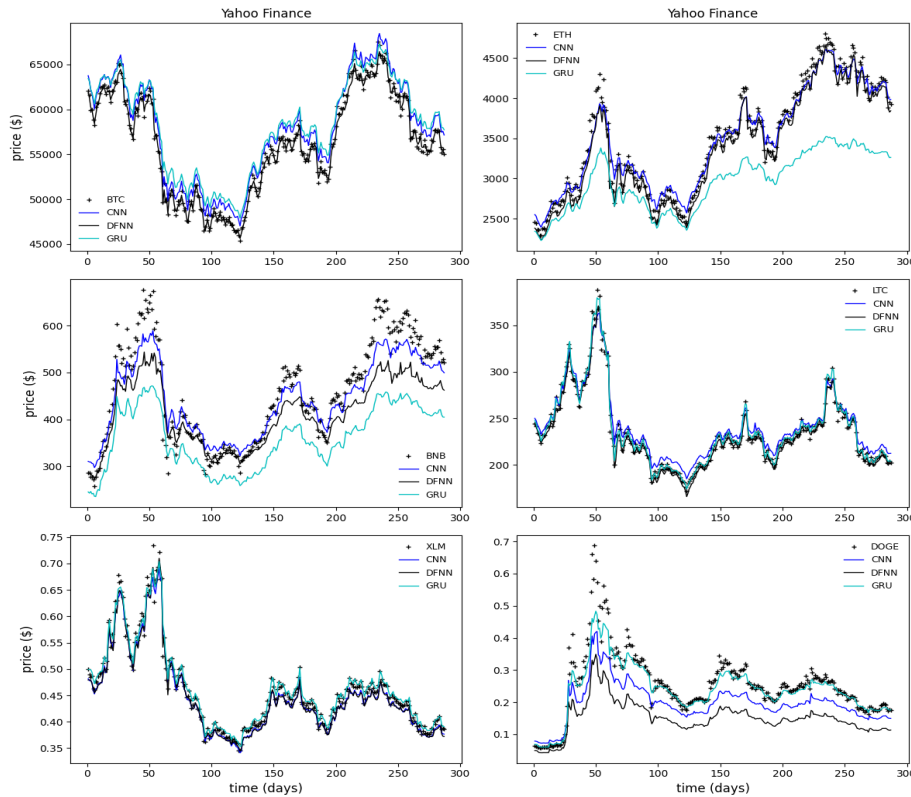
617  
618  
619  
620  
621

Fig. 3. The plot of residuals against predicted closing prices (Scenario A- deep learning models) for the cryptocurrencies. The models' predictions are on the x-axis, and the residuals are on the y-axis.



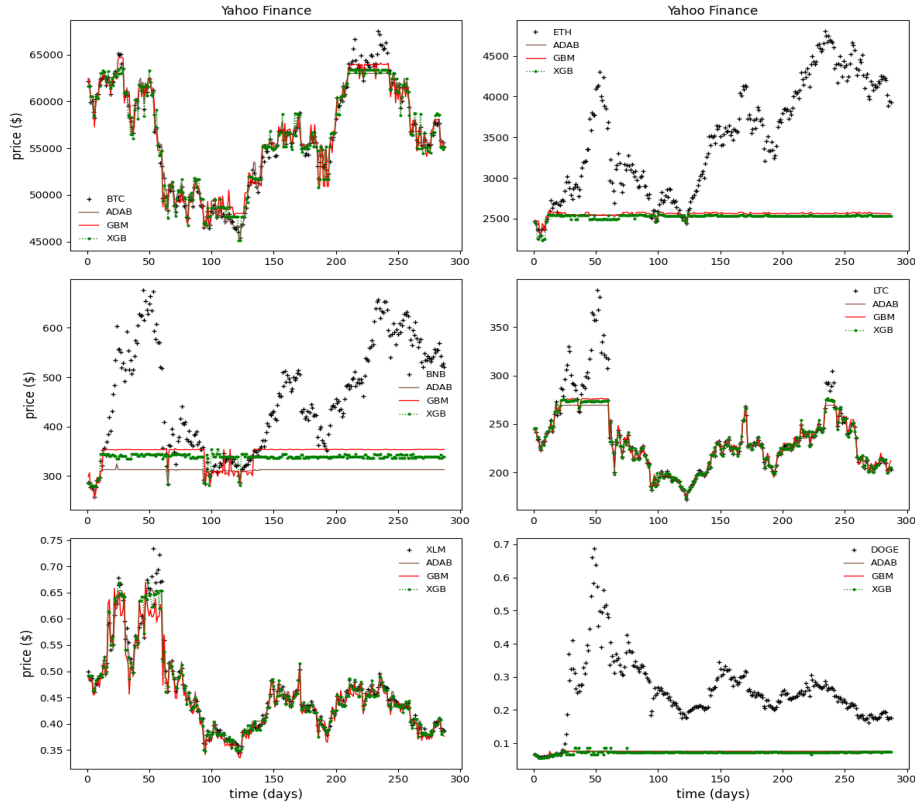
622  
623

Fig. 4. The plot of residuals (tree-based models) against predicted closing prices (Scenario A) of cryptocurrencies



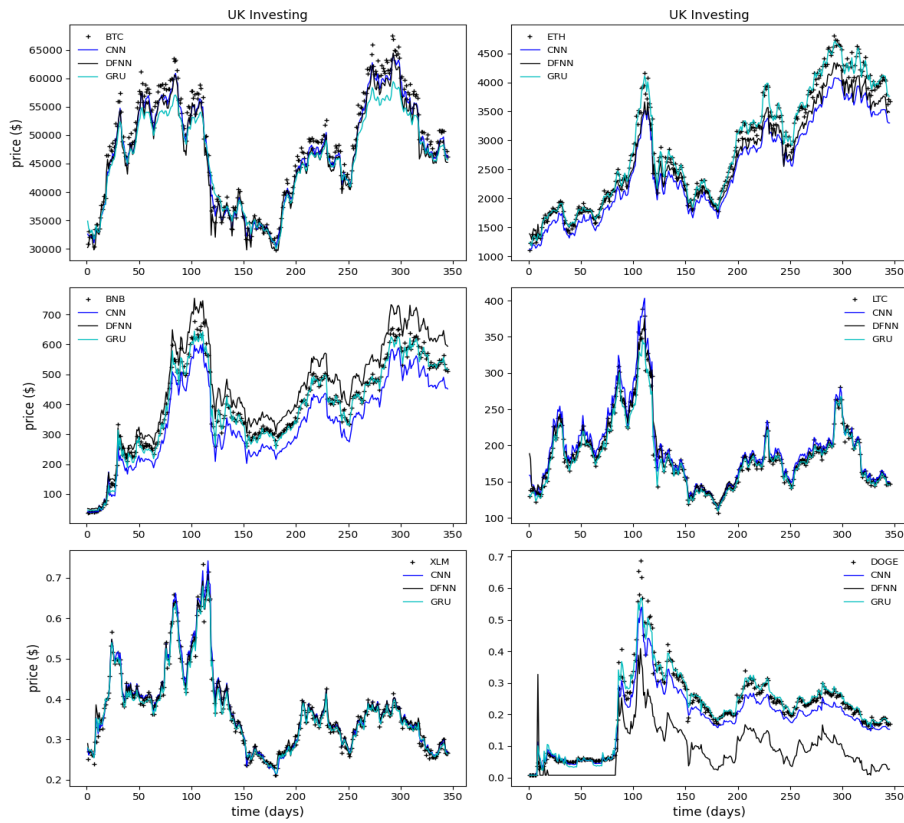
624  
625

Fig. 5. Scenario A: Daily variation of estimated closing prices (Yahoo finance) of DL models compared with measured values



626  
627

Fig. 6. Scenario A: Predicted daily closing prices (Yahoo finance) from tree-based models



628  
629

Fig. 7. Estimated daily closing price predictions of DL models (UK Investing- Scenario B)

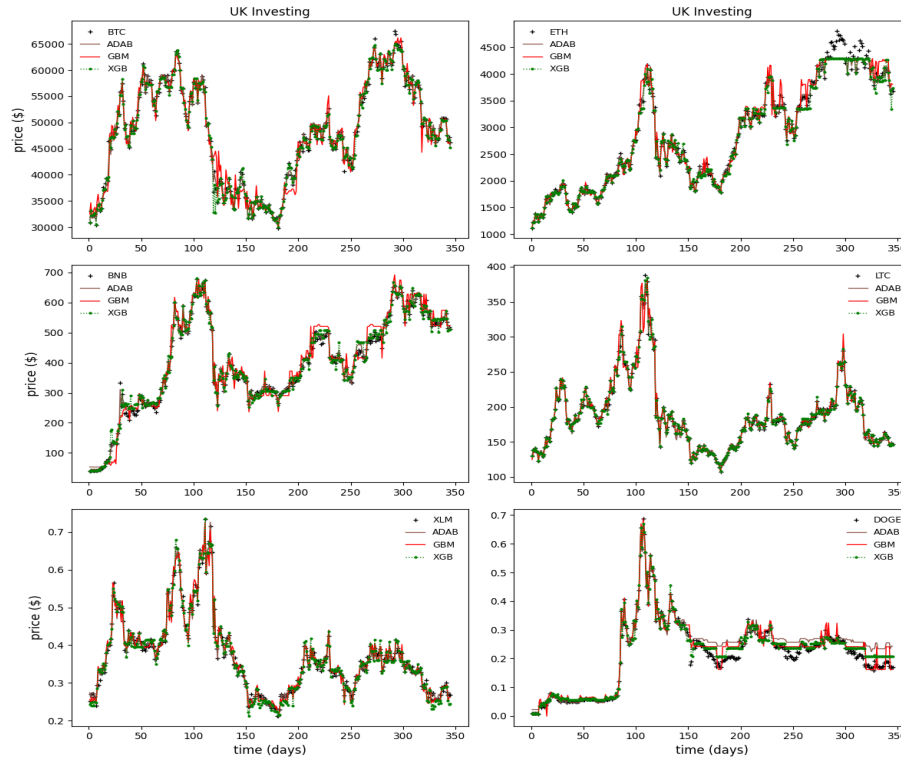


Fig. 8. Estimated daily closing price predictions of boosted tree models (UK Investing- Scenario B)

630  
631  
632  
633  
634  
635  
636  
637  
638  
639  
640  
641  
642  
643

Also, in Fig. 10, black contours indicate the centered RMSE between the predictions and observed values, and this RMSE is proportional to the marked point “observed” on the x-axis. Predictions (Fig. 10) correspond well with observed values (lying nearest to the red arc marked “observed”) and have high correlation and low RMSEs. It can be deduced from Fig. 10 that predictions of models agree best with measured closing prices.

Thus, for most cryptocurrencies (Scenario A), the CNN, GRU, and DFNN models produce high correlation coefficients, low RMSE, and standard deviations from the measured observations, compared to tree-based models that did not work effectively for some cryptocurrencies due to the presence of noisy random features and extreme volatility. Hence, DL techniques are more reliable when the training data is limited or when peaks and drops in crypto prices are inadequately captured.

#### 4.1. Comparison with results in the literature

A comparison of the result obtained by the optimal configuration in this paper and a few other studies (Chowdhury *et al.*, 2020; Dutta *et al.*, 2019; Lahmiri & Bekiros, 2019; Mudassir *et al.*, 2020) listed in Table 1, especially those related to prediction/regression problems regarding the daily Bitcoin price prediction is presented. Furthermore, a Root Mean

Square Error metric,  $RMSE = \sqrt{\frac{\sum_{j=1}^n (o_j - y_j)^2}{n}}$ , is adopted in comparing the results since all these studies utilized RMSE to measure differences between predicted crypto prices and actual observations. The result summary is presented in Table 5. For example, Chowdhury *et al.* (2020) adopted GBM and ensemble techniques to forecast the BTC/USD closing price and reported an RMSE of 32.86 for the GBM method. Similarly, Dutta *et al.* (2019) obtained RMSE values of 0.03 and 0.02, respectively, for neural networks and LSTM for the BTC closing price prediction.

Also, Lahmiri and Bekiros (2019) and Mudassir *et al.* (2020) used deep learning techniques (i.e., GRNN, LSTM, Stacked ANN) to forecast the BTC/USD price. In Lahmiri and Bekiros (2019), the LSTM and GRNN models obtained RMSE values of 2750 and 8800, respectively, while in Mudassir *et al.* (2020), with the data collection period from

656

657 April 1, 2013, to December 31, 2019, the stacked ANN and LSTM obtained RMSE values of 156.30 and 219.59 (for  
 658 30<sup>th</sup>-day forecast) respectively. However, comparing the result from this study with previous studies such as those  
 659 from Chowdhury *et al.* (2020), Dutta *et al.* (2019), Lahmiri and Bekiros (2019), and Mudassir *et al.* (2020), the RMSE  
 660 values obtained in these studies were higher than an RMSE of 0.01 obtained by the best model, optimal CNN, in this  
 661 study.

662 Thus, the proposed optimal architecture could efficiently model the trends and patterns in these cryptocurrencies and  
 663 produce a more reliable result, especially for the BTC closing price prediction. Consequently, the optimal deep  
 664 learning models, especially the optimal CNN architecture, exhibit an inclusive and exemplary performance in the  
 665 overall prediction of cryptocurrencies' closing prices, an important attribute helpful for the older and well-established  
 666 financial markets (stock, forex, commodities) with same complexity characteristics, i.e., volatility clustering, non-  
 667 linear correlations, effects resembling fractality and multifractality (Wątarek *et al.*, 2021).

668  
 669  
 670 Table 6. Comparison with existing studies

Existing study	Model	RMSE	Cryptocurrency
Chowdhury <i>et al.</i> (2020)	GBM	32.86	BTC
Dutta <i>et al.</i> (2019)	Neural networks	0.03	BTC
	LSTM	0.02	
Lahmiri & Bekiros (2019)	LSTM	2750.00	BTC
	GRNN	8800.00	
Mudassir <i>et al.</i> (2020)	Stacked ANN	156.30	BTC
	LSTM	219.59	
Present study	optimized CNN	<b>0.03</b>	BTC
	Optimized GRU	<b>0.02</b>	BTC

671

672

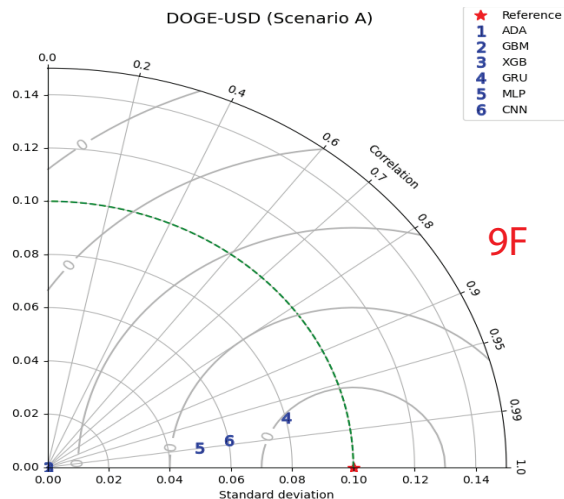
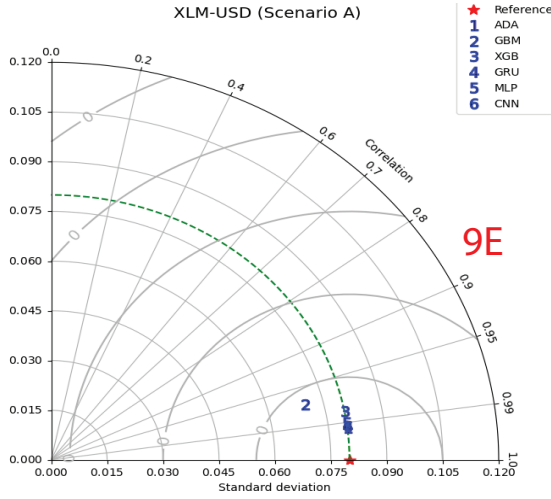
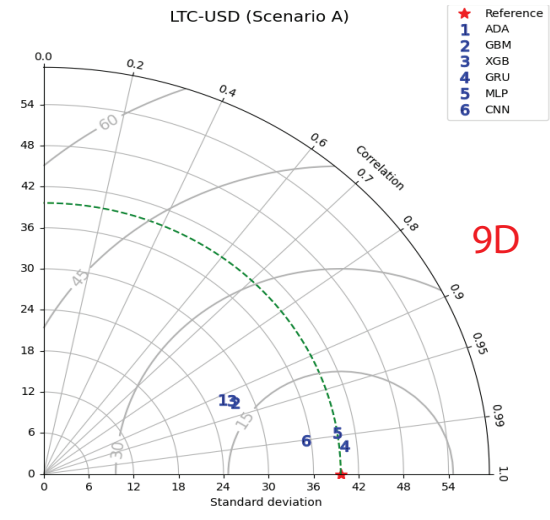
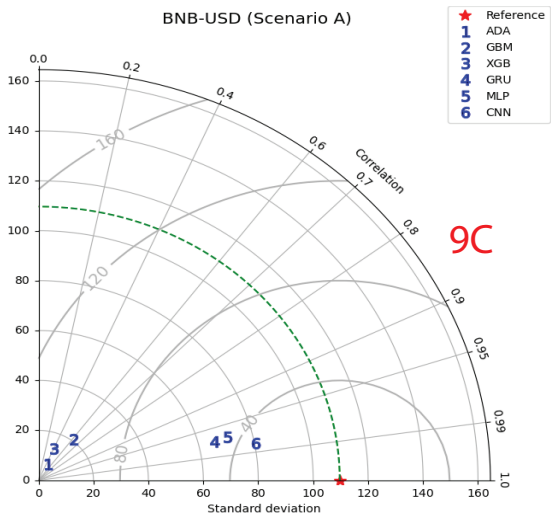
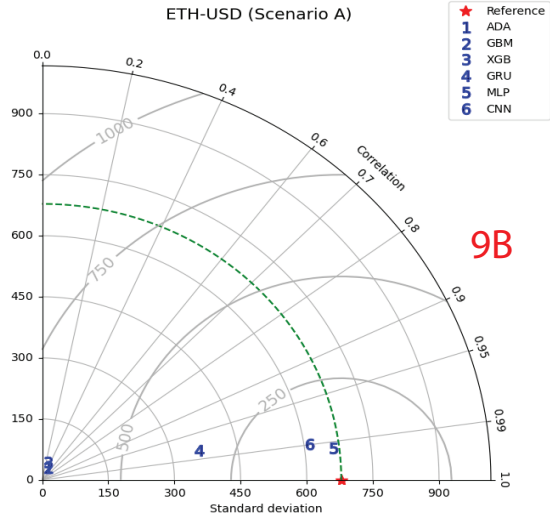
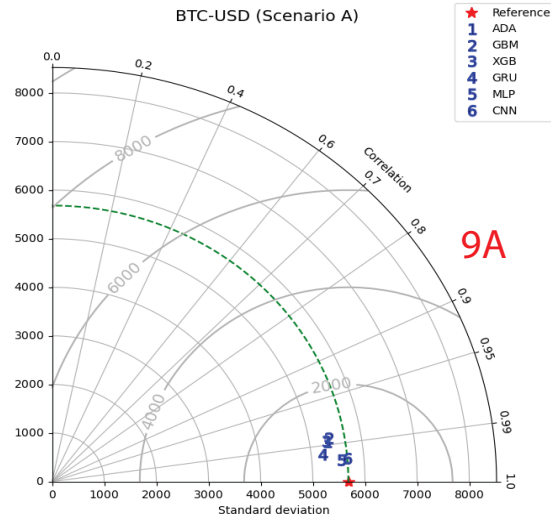
#### 673 4.2. Implication for study

674

675 The results of this research are two-fold: (1) in creating predictive models based on advanced ML methods for  
 676 modeling the crypto market to lower investment risks, and (2) suggesting an optimal configuration for the predictive  
 677 analytics models to forecast the daily closing price of any cryptocurrency efficiently. The previous studies in the area  
 678 mainly focus on a single historical data source for training, validating, and testing their models. Also, they use ML  
 679 models to predict famous and single cryptocurrency platforms. To the best of our knowledge, this study is the first to  
 680 forecast daily closing prices by benchmarking the robustness of DL and boosted tree techniques in terms of using an  
 681 optimal model's configuration across several cryptocurrencies. Also, to guarantee the effectiveness of the models, a  
 682 genetic algorithm is utilized to determine their optimal configurations, including the number of neurons in the hidden  
 683 layers, batch size, and the learning rate. In addition, the performance of prediction models on three different testing  
 684 sets was investigated, and their sensitivity to the training data, where peaks and drops in prices are not adequately  
 685 captured in training sets, was evaluated. Unlike previous studies, a report detailing the conservative estimate of the  
 686 explained variances using four statistical metrics (EVS, MAPE, t-tests, and NSV) and graphical plots (residuals,  
 687 Taylor diagram, time variation plots) was presented. Thus, this study's results can help make futuristic plans to  
 688 minimize risks and uncertainties and increase investment returns.

689

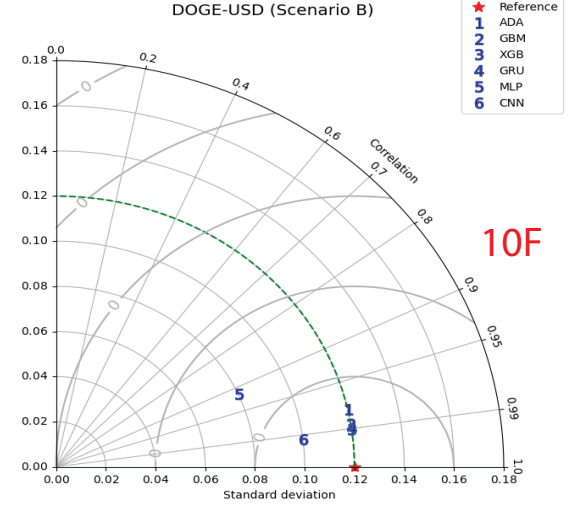
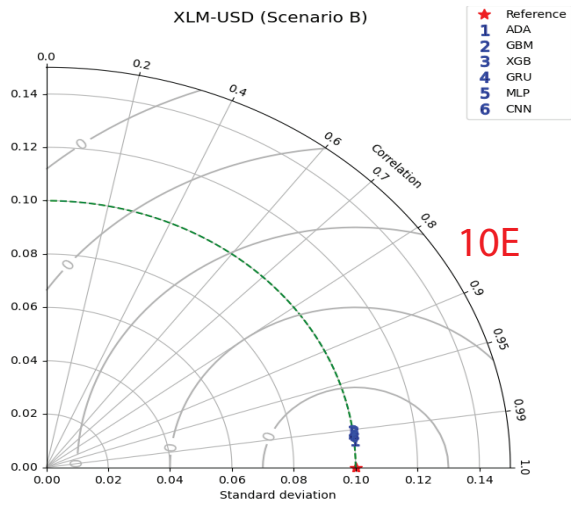
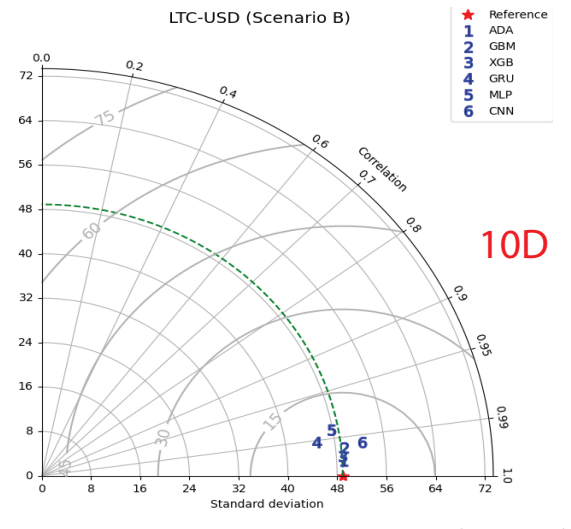
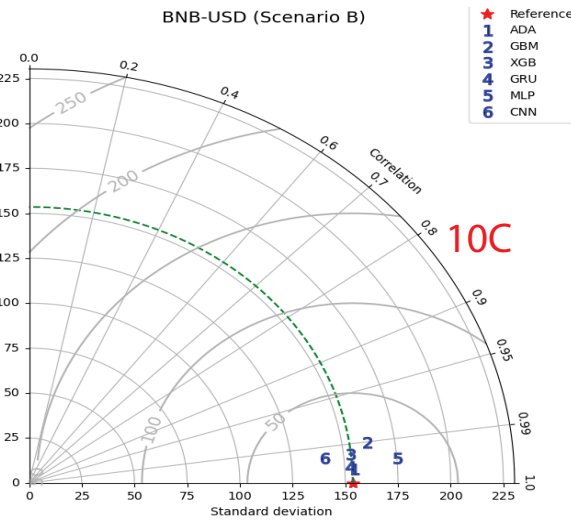
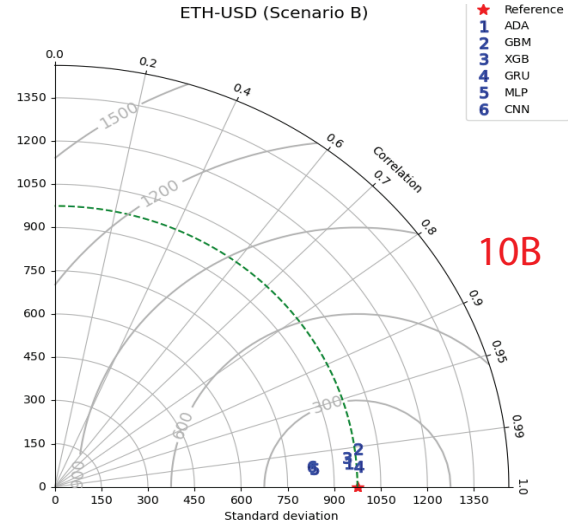
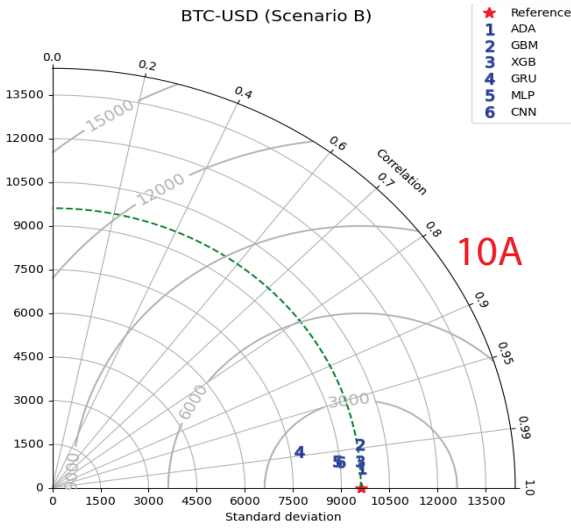
690



691  
 692  
 693

Fig. 9. Taylor's diagram showing a statistical comparison between forecasts and measured values (Yahoo finance)





694  
695  
696  
697  
698

Fig. 10. Taylor's diagram showing a statistical comparison between forecasts and measured values (UK Investing)

## 699 5. Conclusion

700 Forecasting the cryptocurrencies market is a challenging task in finance and a concern to investors due to its high  
701 volatile behavior. Therefore, this paper proposes a robust and optimal predictive models' configuration that can predict  
702 cryptocurrency closing prices with a training set having significant peaks and drops in prices not captured. Thus, the  
703 study benchmarks DL and boosted tree-based techniques, using the models' optimal configurations to predict the daily  
704 closing prices of six different cryptocurrencies datasets collected from more than one data source. Based on the  
705 prediction results achieved in the present study, the following conclusions can be drawn, given a limited training data  
706 sample:

- 707 1 The DL techniques obtain a more significant EVS percentage (between 88% to 98%), indicating that they  
708 have accounted for the total variance in the observed data. However, the boosting trees techniques struggle  
709 to predict daily closing prices for ETH, BNB, and DOGE cryptocurrencies due to the missing insights from  
710 the training set. However, the CNN model produces more accurate results than other DL techniques.
- 711 2 In comparing the robustness of the models on the different test datasets (Yahoo finance, UK investing, and  
712 Bitfinex), DL models (CNN and GRU) on average, produce consistent and higher EVS values ( $0.92 \leq \text{EVS}$   
713  $\leq 0.98$ ) compared to boosted tree-based models, which are low in some cases ( $0.03 \leq \text{EVS} \leq 0.50$ ) for ETH  
714 and DOGE, thus showing the unreliability of the predicted regression for these group of cryptocurrencies  
715 when certain information is missing from the training set.
- 716 3 For Scenario A, the CNN model has the smallest average MAPE of 9%, followed by GRU with an average  
717 MAPE of 11%, GBM (an average MAPE of 17%), DFNN (18%), XGB (average MAPE of 18%), and ADAB  
718 (average MAPE index of 18%).
- 719 4 The residuals from the DL techniques are randomly distributed around the zero horizontal lines, thus  
720 exhibiting no defined patterns, and satisfying the assumption of residuals having a constant variance.  
721 However, residuals from the boosted tree-based counterparts are either not symmetric to the origin or  
722 randomly distributed due to peaks and falls of crypto prices not adequately captured in the training sets.  
723 Hence, their inability to learn from limited examples and generalize some degree of knowledge in predicting  
724 closing prices in this scenario.
- 725 5 The CNN optimal model configuration produces high correlation coefficients, low RMSE, and standard  
726 deviations from the measured observations for most cryptocurrencies. Hence, it is more reliable for limited  
727 training data or when peaks and drops in crypto prices are inadequately captured in the training data. Hence,  
728 CNN is efficient and readily generalizable to predict any cryptocurrency's daily closing price.
- 729 6 This study has revealed the possibility of a single and optimal model's architecture for predicting the prices  
730 of multiple cryptocurrencies. Though, predicting the financial market is difficult due to its complex systems  
731 dynamics. However, deep learning techniques have been the modern approaches to modeling this market.  
732 For instance, deep learning architectures have been applied for stock market prediction (Nelson et al., 2017;  
733 Ticknor, 2013), forex market prediction (Hadizadeh Moghaddam & Momtazi, 2021; Ni et al., 2019), and  
734 commodity market volatility prediction (Kamdern et al., 2020). In the same vein, the computationally  
735 efficient deep learning models developed in this study, especially the optimized CNN model, can be adapted  
736 with little modifications to other financial markets (i.e., stock, bond rates, forex, commodities).

737

## 738 References

- 739 Ajayi, A., Oyedele, L., Akinade, O., Bilal, M., Owolabi, H., Akanbi, L., & Davila-Delgado, J. (2020). Optimised big  
740 data analytics for health and safety hazards prediction in power infrastructure operations. *Safety Science*, 125.  
741 <https://doi.org/https://www.sciencedirect.com/science/article/pii/S0925753520300539>
- 742 Alonso-Monsalve, S., Suárez-Cetrulo, A., Cervantes, A., & Quintana, D. (2020). Convolution on neural networks  
743 for high-frequency trend prediction of cryptocurrency exchange rates using technical indicators. *Expert*  
744 *Systems with Applications*, 149(2020.113250).
- 745 Atsalakis, G. S., Atsalaki, I. G., Pasiouras, F., & Zopounidis, C. (2019). Bitcoin price forecasting with neuro-fuzzy  
746 techniques. *European Journal of Operational Research*, 276(2), 770–780.

- 747 Borges, T., & Neves, R. (2020). Ensemble of machine learning algorithms for cryptocurrency investment with  
748 different data resampling methods. *Applied Soft Computing Journal*, 90(106187).  
749 10.1016/j.asoc.2020.106187
- 750 Canh, N. P., Wongchoti, U., Thanh, S. D., & Thong, N. T. (2019). Systematic risk in cryptocurrency market:  
751 Evidence from DCC-MGARCH model. *Finance Research Letters*, 29, 90–100.  
752 <https://doi.org/10.1016/J.FRL.2019.03.011>
- 753 Chaim, P., & Laurini, M. P. (2019). Nonlinear dependence in cryptocurrency markets. *The North American Journal*  
754 *of Economics and Finance*, 48, 32–47.
- 755 Chen, Z., Li, C., & Sun, W. (2020). Bitcoin price prediction using machine learning: An approach to sample  
756 dimension engineering. *Journal of Computational and Applied Mathematics*, 365, 112395.  
757 0.1016/j.cam.2019.112395
- 758 Cherati, M. R., Haeri, A., & Ghannadpour, S. F. (2021). Cryptocurrency direction forecasting using deep learning  
759 algorithms. *Journal of Statistical Computation and Simulation*, 91(12), 2475–2489.
- 760 Choo, K. K. R. (2015). Cryptocurrency and Virtual Currency: Corruption and Money Laundering/Terrorism  
761 Financing Risks? *Handbook of Digital Currency: Bitcoin, Innovation, Financial Instruments, and Big Data*,  
762 283–307
- 763 Chowdhury, R., Rahman, M., Rahman, M., & Mahdy, M. (2020). An approach to predict and forecast the price of  
764 constituents and index of cryptocurrency using machine learning. *Physica A. Statistical Mechanics and Its*  
765 *Applications*, 551, 124569. 10.1016/j.physa.2020.124569
- 766 Dutta, A., Kumar, S., & Basu, M. (2019). A gated recurrent unit approach to Bitcoin price prediction. *Journal of*  
767 *Risk and Financial Management*, 13(23), 1–16.
- 768 Guo, T., Bifet, A., & Antulov-Fantulin, N. (2018). Bitcoin Volatility Forecasting with a Glimpse into Buy and Sell  
769 Orders. *IEEE International Conference on Data Mining (ICDM)*, 989–994.
- 770 Hadizadeh Moghaddam, A., & Momtazi, S. (2021). Image processing meets time series analysis: Predicting Forex  
771 profitable technical pattern positions. *Applied Soft Computing*, 108, 107460.
- 772 Hastie, T., Tibshirani, R., & Friedman, J. (2009). *The Elements of Statistical Learning: data mining, inference, and*  
773 *prediction*. Springer.
- 774 Huang, J. Z., Huang, W., & Ni, J. (2019). Predicting Bitcoin returns using high-dimensional technical indicators.  
775 *The Journal of Finance and Data Science*, 5(3), 140–155.
- 776 Ibrahim, A., Kashef, R., & Corrigan, L. (2021). Predicting market movement direction for bitcoin: A comparison of  
777 time series modeling methods. *Computers & Electrical Engineering*, 89, 106905.  
778 <https://doi.org/10.1016/J.COMPELECENG.2020.106905>
- 779 Jang, H., & Lee, J. (2018). An empirical study on modeling and prediction of Bitcoin prices with Bayesian neural  
780 networks based on blockchain information. *IEEE Access*, 6, 5427–5437.
- 781 Kristjanpoller, W., & Minutolo, M. C. (2018). A hybrid volatility forecasting framework integrating GARCH,  
782 artificial neural network, technical analysis and principal components analysis. *Expert Systems with*  
783 *Applications*, 109, 1–11.
- 784 Kwon, D., Kim, J., Heo, J., Kim, C., & Han, Y. (2019). Time series classification of cryptocurrency price trend  
785 based on a recurrent LSTM neural network. *Journal of Information Processing Systems*, 15(3), 694–706.
- 786 Lahmiri, S., Bekiros, S., & Salvi, A. (2018). Long-range memory, distributional variation and randomness of bitcoin  
787 volatility. *Chaos, Solitons & Fractals*, 107, 43–48.
- 788 Lahmiri, S., & Bekiros, S. (2019). Cryptocurrency forecasting with deep learning chaotic neural networks *Chaos*.  
789 *Chaos, Solitons & Fractals*, 118, 35–40.
- 790 Lahmiri, S., & Bekiros, S. (2020a). Big data analytics using multi-fractal wavelet leaders in high-frequency Bitcoin  
791 markets. *Chaos, Solitons & Fractals*, 131, 109472. <https://doi.org/10.1016/J.CHAOS.2019.109472>
- 792 Lahmiri, S., & Bekiros, S. (2020b). Intelligent forecasting with machine learning trading systems in chaotic intraday  
793 Bitcoin market *Chaos, Solitons & Fractals*, 133, 109641. 10.1016/j.chaos.2020.109641
- 794 LeCun, Y., Bengio, Y., & Hinton, G. (2015). Deep learning. *Nature*, 521(7553), 436–444.
- 795 Li, T., Chamrajnagar, A., Fong, X., Rizik, N., & Fu, F. (2018). Sentiment-based prediction of alternative  
796 cryptocurrency price fluctuations using gradient boosting tree model. *Frontiers in Physics*, 7(98), 1–8.
- 797 Mallqui, D., & Fernandes, R. (2019). Predicting the direction, maximum, minimum and closing prices of daily  
798 Bitcoin exchange rate using machine learning techniques. *Applied Soft Computing Journal*, 75, 596–606.
- 799 Miura, R., Pichl, L., & Kaizoji, T. (2019). Artificial neural networks for realized volatility prediction in  
800 cryptocurrency time series. *International Symposium on Neural Networks*, 165–172.

801 Mudassir, M., Bennbaia, S., Unal, D., & Hammoudeh, M. (2020). Time-series forecasting of Bitcoin prices using  
802 high-dimensional features: a machine learning approach. *Neural Computing and Applications*, 1–15.  
803 <https://doi.org/10.1007/S00521-020-05129-6/FIGURES/10>  
804 Nakano, M., Takahashi, A., & Takahashi, S. (2018). Bitcoin technical trading with artificial neural network. *Physica*  
805 *A. Statistical Mechanics and Its Applications*, 510, 587–609.  
806 Nelson, D., Pereira, A., & de Oliveira, R. (2017). Stock market's price movement prediction with LSTM neural  
807 networks. *International Joint Conference on Neural Networks*, 1419–1426.  
808 Ni, L., Li, Y., Wang, X., Zhang, J., Yu, J., & Qi, C. (2019). Forecasting of Forex Time Series Data Based on Deep  
809 Learning. *Procedia Computer Science*, 147, 647–652.  
810 Peng, Y., Albuquerque, P. H. M., Camboim de Sá, J. M., Padula, A. J. A., & Montenegro, M. R. (2018). The best of  
811 two worlds: Forecasting high frequency volatility for cryptocurrencies and traditional currencies with Support  
812 Vector Regression. *Expert Systems with Applications*, 97, 177–192.  
813 Poongodi, M., Sharma, A., Vijayakumar, V., Bhardwaj, V., Sharma, A. P., Iqbal, R., & Kumar, R. (2020).  
814 Prediction of the price of Ethereum blockchain cryptocurrency in an industrial finance system. *Computers &*  
815 *Electrical Engineering*, 81, 106527. <https://doi.org/10.1016/J.COMPELECENG.2019.106527>  
816 Kamdem, S.J., Essomba, R.B., & Berinyuy, J.N. (2020). Deep learning models for forecasting and analyzing the  
817 implications of COVID-19 spread on some commodities markets volatilities. *Chaos, Solitons & Fractals*, 140,  
818 110215. <https://doi.org/10.1016/J.CHAOS.2020.110215>  
819 Shah, D., & Zhang, K. (2014). Bayesian regression and Bitcoin. *52nd Annual Allerton Conference on*  
820 *Communication, Control, and Computing*, 409–414.  
821 Sheridan, R., Wang, W., Liaw, A., Ma, J., & Gifford, E. (2016). Extreme Gradient Boosting as a Method for  
822 Quantitative Structure-Activity Relationships. *Journal of Chemical Information and Modeling*, 56(12), 2353–  
823 2360.  
824 Ticknor, J. L. (2013). A Bayesian regularized artificial neural network for stock market forecasting. *Expert Systems*  
825 *with Applications*, 40(14), 5501–5506.  
826 Wątarek, M., Drożdż, S., Kwapien, J., Minati, L., Oświęcimka, P., & Stanuszek, M. (2021b). Multiscale  
827 characteristics of the emerging global cryptocurrency market. *Physics Reports*, 901, 1–82.  
828 Sun, X, Liu, M., & Zeqian, S. (2020). A novel cryptocurrency price trend forecasting model based on LightGBM.  
829 *Finance Research Letters*, 32, 101084. <https://doi.org/10.1016/J.FRL.2018.12.032>  
830 Zoumpikas, T., Houstis, E., & Vavalis, M. (2020). ETH analysis and predictions utilizing deep learning. *Expert*  
831 *Systems with Applications*, 162(30), 113866β